Molecular dynamics of the rough sphere fluid. I. Rotational relaxation*

J. O'Dell[†] and Bruce J. Berne

Department of Chemistry, Columbia University, New York, New York 10027

A systematic study is made of rotational relaxation in rough sphere fluids for densities ranging from 0.1 to 0.666 of the closest packed density. Many of the current models of rotational relaxation are tested against the results of molecular dynamics. It is found that for densities higher than 0.40 of the closest packed density only the Fokker–Planck model is consistent with experiment. The various extended diffusion models, the jump diffusion model, and the rotational diffusion model are not only internally inconsistent, but also do not agree with experiment. No theory is consistent with experiment at intermediate densities where the collisional and the inertial time scales are comparable. In addition to the foregoing, it appears that the rough spheres tumble more freely in the solid state than they do in the fluid state at the melting density.

I. INTRODUCTION

Much of what is known about the structural and dynamical properties of fluids springs from the study of the properties of the smooth hard sphere fluid. This model has played a central role in the development of the kinetic theory of gases. The structure of the hard sphere fluid has exercised many an able theorist. Recently it has been found that the hard sphere fluid provides an excellent reference system for "thermodynamic perturbation theory" in the calculation of the structure of more realistic fluids.[1] It is hoped that perturbation theories of transport properties will be forthcoming in the near future.[2]

In recent years the smooth hard sphere fluid has been studied in great detail using the two major techniques of numerical statistical mechanics: Monte Carlo studies of the static properties and molecular dynamics studies of both the static and time dependent properties. Such studies have shown that the hard sphere fluid in two and three dimensions undergoes a liquid–solid phase transition.[3] More important perhaps is the discovery that those time correlation functions whose time integrals determine the transport coefficients (through the Kubo relations) depend asymptotically on time as $t^{-d/2}$, where d is the dimensionality.[3,4] On further investigation it appears that Lennard–Jones fluids also exhibit this behavior. This discovery has rather profound implications. It means that transport coefficients diverge in two dimensional fluids, and concommitantly that the equations of fluid mechanics can not apply to such systems. Furthermore, the Burnett coefficients diverge in three dimensions.[3] This has led to much feverish theoretical activity which has resulted in part in correcting the time honored Boltzmann and Enskog equations of the kinetic theory of gases to include correlated binary collisions.[5] The "new kinetic theory" that has resulted gives complete agreement with the computer experiments in that it predicts the $t^{-d/2}$ dependence.

Two important conclusions are immediately apparent. Because of its simplicity, the hard sphere fluid has been very productive in conjunction with computer experiments in advancing our knowledge of the fluid state and in pointing in the direction of future developments in analytical theories. The properties of these fluids are often found in more realistic fluids.

Until recently, much of the activity in the theory of fluids has centered around studies of simple fluids whose molecules have no internal degrees of freedom. Yet polyatomic fluids are of considerable interest in chemistry and physics. The whole question of rotational and vibrational relaxation and energy transfer in fluids is of enormous interest to a wide range of scientists. In addition, the question of molecular reorientations is very important to the understanding of many forms of spectroscopy such as infrared, microwave, Raman, Rayleigh, depolarization of fluorescence, picosecond absorption, dielectric relaxation, and thermal neutron scattering. Nevertheless, there has been no systematic study of such fluids from a theoretical point of view.[6]

This paper represents the first of a series of papers devoted to a systematic study of fluids containing rigid molecules. We begin with a study of the *rough sphere fluid*, although this series is by no means limited to this system. It is our hope that this model will be as revealing about the relaxation properties of molecular fluids as the smooth sphere fluid has been about the properties of simpler fluids. One of the useful features of the rough sphere fluid is that its structure is identical to that of the smooth sphere fluid at the same density. Thus, information already obtained in previous studies is of use to us here.

The rough sphere model of molecular collisions has a long history.[7] It was first proposed by Pidduck, and was later explored by Chapman and Cowling. The rough sphere is perhaps the simplest particle that has rotational degrees of freedom. A collision between two rough spheres is instantaneous (of zero duration). During this collision, the relative velocity of the points of contact of two spheres is completely inverted. Thus, one sphere can transfer not only linear momentum but also spin angular momentum to the other sphere. Obviously, many features of the rough sphere fluid will differ from those of the smooth sphere fluid.

There are several questions that can be posed about these fluids. For example, (a) how are the transport coefficients modified by roughness? (b) is there any

long time persistence in the spin angular velocity or orientations? (c) is the kinetics of the melting transition altered by roughness? Although we believe that these are interesting questions, we shall not discuss them in this first paper. Rather we shall focus our attention on the problem of *rotational diffusion* in these fluids. In addition, some attention is given to translational self-diffusion.

There exist several important theories of molecular reorientations. Oldest and best known is the theory of rotational diffusion—a small step random walk model—put forth by Debye.[8]

Ivanov extended the Debye model by developing the jump diffusion model in which a molecule is assumed to be locked into place between reorienting jumps.[9] The two quantities of interest here are the mean time between jumps and the distribution of jump angles. When only small angles are allowed, this model reduces to the Debye model. This model is often invoked for reorientation in solids where activated jumps can be envisioned and for hydrogen bonded solutions. We do not expect it to be relevant to our studies of the rough sphere fluid. More recently, Gordon has developed a very simple and appealing extended diffusion model in which each molecule is regarded as rotating freely between instantaneous collisions.[10] A collision merely either (a) randomizes the direction of the rotational angular momentum (M diffusion), or (b) randomizes (thermalizes) both the direction and magnitude of the angular momentum (J diffusion). Gordon further assumes that successive binary collisions are uncorrelated. The chief result of the Gordon theory is embodied in a relation between the orientational correlation function in the model and the free rotator orientational correlation function.

Only one parameter enters the theory, and that is

$$\beta = (I/kT)^{1/2}(1/t_c) , \qquad (1.1a)$$

where I is the moment of inertia, and t_c is the mean time between collisions. β reflects the ratio of the free rotor tumbling time to the collision time and is expected to be very small for a dilute gas and very large for a dense fluid. Because he applied these models to real systems with continuous pair potentials, where there is no well defined collision time, Gordon treats β as a parameter to be fit to experiment. In the rough sphere fluid there exists a well defined collision time, so that Gordon's ideas[10] can be directly tested.

Recently, Chandler has introduced a model which he claims takes into account all sequences of independent binary collisions.[11] This model gives $C_l(\tau)$ which are identical in functional form to Gordon's J-diffusion model, except that β is now

$$\beta_E = (I/KT)^{1/2} \frac{1}{t_\omega} , \qquad (1.1b)$$

where t_ω is the angular momentum correlation time in the Enskog approximation (hence the subscript E)—a quantity also easily calculated for the rough sphere fluid [see Eq. (3.13b)]. Thus, we can also compare this "Enskog" model with our rough sphere molecular dynamics. It is expected that both of these models will reduce to the Debye model for very large values of β_c or β_E.

The extended diffusion model is very appealing because it incorporates the obvious physical features of orientational relaxation and because it is relatively simple to apply. Nevertheless, for cases in which there is cooperativity in the decay of the angular velocity, this model cannot describe the orientational relaxation. In addition, as will be shown in Sec. III, even in a rough sphere system, the angular velocity cannot be randomized in the collision time.

Fixman and Rider[12] have presented a unified approach to rotational relaxation based on a general Markoffian operator which for instantaneous collisions acts just in angular momentum space. They then showed that the extended diffusion model and various *ad hoc* models were special cases of this general Markoffian theory. This formulation enabled them to generalize the extended diffusion model to cases intermediate between the J- and the M-diffusion model. In addition, Langevin relaxation of the angular velocity could be incorporated and a Brownian motion theory of orientational relaxation could be given. In this way, a Fokker–Planck (F–P) equation[12,13] is derived for the joint orientation and angular momentum distribution function. For a spherical top molecule, only one parameter is needed, and this is the rotational friction constant. For large values of the friction constant this model reduces to the Debye model, but for small values of the friction constant this model, like the above extended diffusion models, also describe the inertial (free rotor) reorientations. In this paper we shall show that for spherical tops, the Fokker–Planck theory[12] is preferable to the extended diffusion model.

Thus, in this first paper in this series, the reorientation of a unit vector u rigidly attached to the center of each of the spheres is studied and the correlation functions

$$C_l(t) \equiv \langle P_l(\mathbf{u}(0) \cdot \mathbf{u}(t)) \rangle \quad l = 1, 2 , \qquad (1.2)$$

where $P_l(x)$ is a Legendre polynomial of order l, are determined. In addition, the autocorrelation functions of the spin angular velocity $\omega(t)$ and the linear velocity $\mathbf{v}(t)$,

$$C_v(t) \equiv \langle \mathbf{v}(0) \cdot \mathbf{v}(t) \rangle \langle v^2 \rangle^{-1} , \qquad (1.3)$$

$$C_\omega(t) \equiv \langle \omega(0) \cdot \omega(t) \rangle \langle \omega^2 \rangle^{-1} , \qquad (1.4)$$

are determined.

These correlation functions are determined for the rough sphere fluid for a series of densities by performing computer experiments on these fluids. The resulting correlation functions are compared with the predictions of the preceding major models of molecular reorientation. In addition, there is some discussion of the Hubbard relation.

The chief conclusions of this study are

(a) No theory is consistent with the molecular dynamics results at all densities. Only at the very highest stable

fluid density does the Hubbard relation[14] apply.

(b) At the melting density, rough spheres reorient more freely in the solid than in the liquid.

(c) Only at the melting density does the Debye theory describe the reorientations.

(d) The angular velocity correlation function always lies above the exponential predicted by the Enskog equation, indicating that at high densities correlated collisions are important even at short times.

(e) There are systematic differences between the experiments and the Enskog theory introduced by Chandler,[11] and these differences are significantly larger than the possible uncertainties in the experimental results.

(f) The Fokker–Planck theory of all the models seems to be in best agreement with experiment.

These conclusions are particularly important with regard to the extended diffusion models,[10] since the collisions between rough spheres are truly instantaneous. Should this model not work for rough spheres, we should have grave reservations about its applicability to realistic fluids.

In order to present our study in a coherent form we outline the simple theories in Sec. II. In Sec. III we discuss some of the analytical features of the rough sphere model, and in Sec. IV, we summarize the methods used in our molecular dynamics study. In Sec. V we compare theory and experiment, and in Sec. VI we discuss the results.

II. THE THEORY OF MOLECULAR REORIENTATION

In this section, several models of rotational relaxation are reviewed and applied to rough spheres.

A. Free rotation

The orientational correlation function of an ideal gas of rough spheres (no collisions) is[15]

$$C_l^{(0)}(t) = \left\langle \frac{1}{2l+1} \sum_{m=-l}^{l} e^{im\omega t} \right\rangle ,$$

where ω is the rotational speed of a sphere and the brackets indicate an average over the Maxwellian distribution $[w(\omega)\,dw = 4\pi(I/2\pi kT)^{3/2}\,\omega^2\,e^{-I\omega^2/2kT}\,d\omega]$. Explicit evaluation of the integral gives

$$C_l^{(0)}(t) = \frac{1}{2l+1} \sum_{m=-l}^{+l} (1 - m^2\tau^2)\,e^{-m^2\tau^2/2} , \qquad (2.1)$$

where τ is the reduced time,

$$\tau \equiv [\tfrac{1}{3}\langle\omega^2\rangle]^{1/2} t = \left(\frac{kT}{I}\right)^{1/2} t , \qquad (2.2)$$

I is the moment of inertia of the particle, and T is the temperature. The free particle correlation functions are denoted by the superscript (0). These functions decay on a time scale $\tau \sim 1$, but finally approach $(2l+1)^{-1}$ rather than zero. This results from the fact that the component of the unit vector along the axis of rotation does not change in time. This projection is given by the $m=0$ term in Eq. (2.1), which is $(2l+1)^{-1}$.

B. Extended diffusion

In the Gordon extended diffusion model,[10] it is assumed that each sphere rotates freely between collisions which are of zero duration. During a collision, the angular velocity discontinuously changes, but a unit vector embedded in the sphere does not reorient at all. Furthermore, it is assumed that successive binary collisions are independent. Gordon discussed two extreme models called the M-diffusion and the J-diffusion models. In the M-diffusion model, each collision randomizes the direction of the angular velocity, leaving its magnitude unchanged; whereas in the J-diffusion model, each collision randomizes both the direction and magnitude of the angular velocity. These two models are sufficiently simple that the orientational correlation functions can be determined for them. First we treat the J-diffusion model.

Let us denote by $C_l(n, \tau)$ the orientational correlation function for the subset of molecules that have undergone $n-1$ collisions in the (reduced) time τ irrespective of the precise times of these collisions. Furthermore, let us assume that this function is weighted by the fraction of particles that have undergone $n-1$ collisions in τ. Then, for example, $C_l(1, \tau)$ is the weighted correlation function for a particle to undergo zero collisions in the time τ. $C_l(1, \tau)$ is consequently the free particle correlation function $C_l^{(0)}(\tau)$ weighted by the probability that a particle will not suffer a collision in the time τ. Because the model postulates that the successive collisions are uncorrelated, the weighting factor is $e^{-\tau/\tau_c}$, where τ_c is the mean time between collisions or "the collision time" (in reduced units). Thus,

$$C_l(1, \tau) = e^{-\tau/\tau_c} C_l^{(0)}(\tau) . \qquad (2.3)$$

To proceed, we note that

$$C_l(n+1, \tau) = \int_0^\tau C_l(1, \tau - \tau') \frac{d\tau'}{\tau_c} C_l(n, \tau') . \qquad (2.4)$$

The integrand is simply the contribution to $C_l(n+1, \tau)$ from those particles which suffer $n-1$ collisions in time τ', suffer the next collision between τ' and $\tau' + d\tau'$, and then rotate freely for the time $\tau - \tau'$. The factor $d\tau'/\tau_c$ is the probability of a collision between τ' and $\tau' + d\tau'$. Clearly, τ' can occur anywhere between 0 and t—hence the integration. Laplace transformation of Eq. (2.4) yields

$$\bar{C}_l(n+1, p) = \beta \bar{C}_l(1, p)\bar{C}_l(n, p) , \qquad (2.5)$$

where the convolution theorem has been used, p is the Laplace variable, and β is the parameter

$$\beta \equiv 1/\tau_c . \qquad (2.6)$$

The Laplace transform of Eq. (2.3) gives $\bar{C}_l(1, p) = \bar{C}_l^{(0)}(p + \beta)$. Substitution of this into Eq. (2.5) followed by iteration yields

$$\bar{C}_l(n+1, p) = [\beta \bar{C}_l^{(0)}(p + \beta)]^n \bar{C}_l^{(0)}(p + \beta) . \qquad (2.7)$$

It is clear that $C_l(\tau)$ can be found by summing $C_l(n+1, \tau)$ from $n=0$ to ∞; that is, over all numbers of collisions so that $C_l(\tau) = \sum_{n=0}^{\infty} C_l(n+1, \tau)$. Likewise for the Laplace transform. Thus, for J diffusion,

$$\tilde{C}_l(p) = \sum_{n=0}^{\infty} \left[\beta \tilde{C}_l^{(0)}(p+\beta) \right]^n \tilde{C}_l^{(0)}(p+\beta) , \qquad (2.8a)$$

$$\tilde{C}_l(p) = \tilde{C}_l^{(0)}(p+\beta)/\left[1 - \beta \tilde{C}_l^{(0)}(p+\beta) \right] , \qquad (2.8b)$$

where the last equation results from an explicit summation of the geometric series. Equation (2.8b) is the chief result of the Gordon theory, although it was originally expressed in this form elsewhere.[16] According to Eq. (2.8b), the Laplace transform of $C_l(\tau)$ is determined completely by the parameter β and the free particle correlation function $C_l^{(0)}(\tau)$—through its transform

$$\tilde{C}_l^{(0)}(p+\beta) = \int_0^{\infty} d\tau e^{-(p+\beta)\tau} C_l^{(0)}(\tau) . \qquad (2.9)$$

Substitution of Eq. (2.1) followed by integration gives

$$\tilde{C}^{(0)}(p+\beta)$$

$$= \frac{1}{2l+1} \left\{ 2 \sum_{m=1}^{l} \left(\frac{p+\beta}{m}\right)\left[1 - \left(\frac{p+\beta}{m}\right) f\left(\frac{p+\beta}{m}\right)\right] + \frac{1}{p+\beta} \right\} ,$$

$$(2.10a)$$

where

$$f(x) = \left(\frac{\pi}{2}\right)^{1/2} e^{x^2/2} \operatorname{erfc}(x/\sqrt{2}) , \qquad (2.10b)$$

and where erfc denotes the complimentary error function.

The M-diffusion model can be developed along the same lines. Because in this model the angular speed of a sphere does not change from collision to collision, $C_l(n, \tau) = C_l(n, \tau | \omega)$; that is, $C_l(n, \tau)$ is a function of the angular speed. Following the same logic, the M-diffusion correlation function result is

$$\tilde{C}_l(p) = \left\langle \frac{\tilde{C}_l^{(0)}(p+\beta | \omega)}{1 - \tilde{C}_l^{(0)}(p+\beta | \omega)} \right\rangle , \qquad (2.11a)$$

where

$$\tilde{C}_l^{(0)}(p+\beta | \omega) = \frac{1}{2l+1} \sum_{m=-l}^{+l} (p+\beta-im\omega)^{-1} , \qquad (2.11b)$$

and where the brackets indicate an average over the Maxwell distribution function $w(\omega)$.

Fixman and Rider[12] have generalized the extended diffusion model so that situations between the M-diffusion and J-diffusion model can be handled. They define two parameters β_0 and β_1 such that $\beta_0/\beta_0 + \beta_1$ and $\beta_1/\beta_0 + \beta_1$ are, respectively, the probabilities that a collision will equilibrate the rotational kinetic energy distribution and the probability that this will remain unchanged. Thus, if $\beta_1 = 0$, J diffusion should obtain, whereas if $\beta_0 = 0$, M diffusion should obtain. It is possible to express the results of Fixman and Rider in a suggestive form. For this purpose let $\tilde{C}_l(p|\beta)$ and $\tilde{C}_l^{(M)}(p|\beta)$ denote the Laplace transform at Laplace variable p of the orientational correlation function $C_l(\tau)$ in the Fixman and Rider theory and in the M-diffusion theory, respectively, for parameter β. Then we find that

$$\tilde{C}_l(p|\beta_0+\beta_1) = \frac{\tilde{C}_l^{(M)}(p+\beta_0|\beta_1)}{1 - \beta_0 \tilde{C}_l^{(M)}(p+\beta_0|\beta_1)} . \qquad (2.11c)$$

Because $\tilde{C}_l^{(M)}(p|0) = \tilde{C}_l^{(0)}(p)$, this formula correctly reduces to the M- and J-diffusion results in the appropriate limits.

In the following, the J-diffusion model will be used to illustrate some of the techniques that are often used in comparing these extended diffusion models to experiment.

A parameter often discussed in the literature is the "*orientational correlation time*" τ_l^* defined by

$$\tau_l^* \equiv \lim_{p \to 0} \int_0^{\infty} dt \, C_l(\tau) e^{-p\tau} = \lim_{p \to 0} \tilde{C}_l(p) . \qquad (2.12)$$

This quantity is the area under $C_l(\tau)$ in reduced time units [in real time, $t_l = \tau_l^*(I/kT)$]. Clearly, τ_l^* can be evaluated explicitly in terms of β by substitution of Eqs. (2.8b), (2.10a), and (2.10b) into Eq. (2.12) and taking the limit $p \to 0$. This gives

$$\tau_l^* = \tilde{C}_l^{(0)}(\beta)/\left[1 - \beta \tilde{C}_l^{(0)}(\beta) \right] , \qquad (2.13a)$$

where

$$C_l^{(0)}(\beta) = \frac{1}{2l+1} \left\{ 2 \sum_{m=1}^{l} \frac{\beta}{m} \left(1 - \frac{\beta}{m} f\left(\frac{\beta}{m}\right)\right) + \frac{1}{\beta} \right\} ,$$

$$(2.13b)$$

where $f(x)$ is defined in Eq. (2.10b).

The only parameter that enters the Gordon theory is β. As mentioned in the introduction, β should increase with density from $\beta = 0$ at $\rho = 0$. The dependence of τ_l^* on β as given by Eq. (2.13) is plotted in Fig. 1 for $l=1$ and $l=2$. It is a simple matter to show that for small β

$$\tau_l^* = \frac{1}{2l} \beta^{-1} \quad \text{(dilute fluid)} , \qquad (2.13c)$$

and for large β

$$\tau_l^* = \frac{1}{l(l+1)} \beta \quad \text{(dense fluids)}. \qquad (2.13d)$$

Figure 2 is rather easy to understand. At zero density, $\beta = 0$, and $C_l(\tau) = C_l^{(0)}(\tau)$. Since $C_l^{(0)}(\tau)$ decays to $(2l+1)^{-1}$ and not zero, its time integral is infinite, thereby leading to $\tau_l^* \to \infty$.

At sufficiently low densities, collisions are sufficiently infrequent that the rotors rotate many cycles between collisions, giving rise to small β. Thus, for times smaller than the collision time β^{-1}, $C_l(\tau)$ behaves like a $C_l^{(0)}(\tau)$. However, for times on the order of β^{-1}, collisions reorient the axis of rotation, thereby giving rise to changes in the projection of u on the rotational axis. Thus, $C_l(\tau)$ should decay to zero for times large compared to β^{-1}; and τ_l^*, the area under $C_l(\tau)$, should be large but finite. Thus, as ρ increases from 0, τ_l^* decreases as predicted by Eq. (2.13c) (see Fig. 1). For very large ρ, collisions are so frequent that u cannot rotate much between collisions. Then $C_l(\tau)$ is expected to decay very slowly with time. This gives rise to a time integral, τ_l^*, which is again very large—hence Eq. (2.13d). The minimum in Fig. 1 occurs at a point where the decay time of the projection of u on the initial rotation axis is approximately the same as the decay time for the components of u perpendicular to this axis.

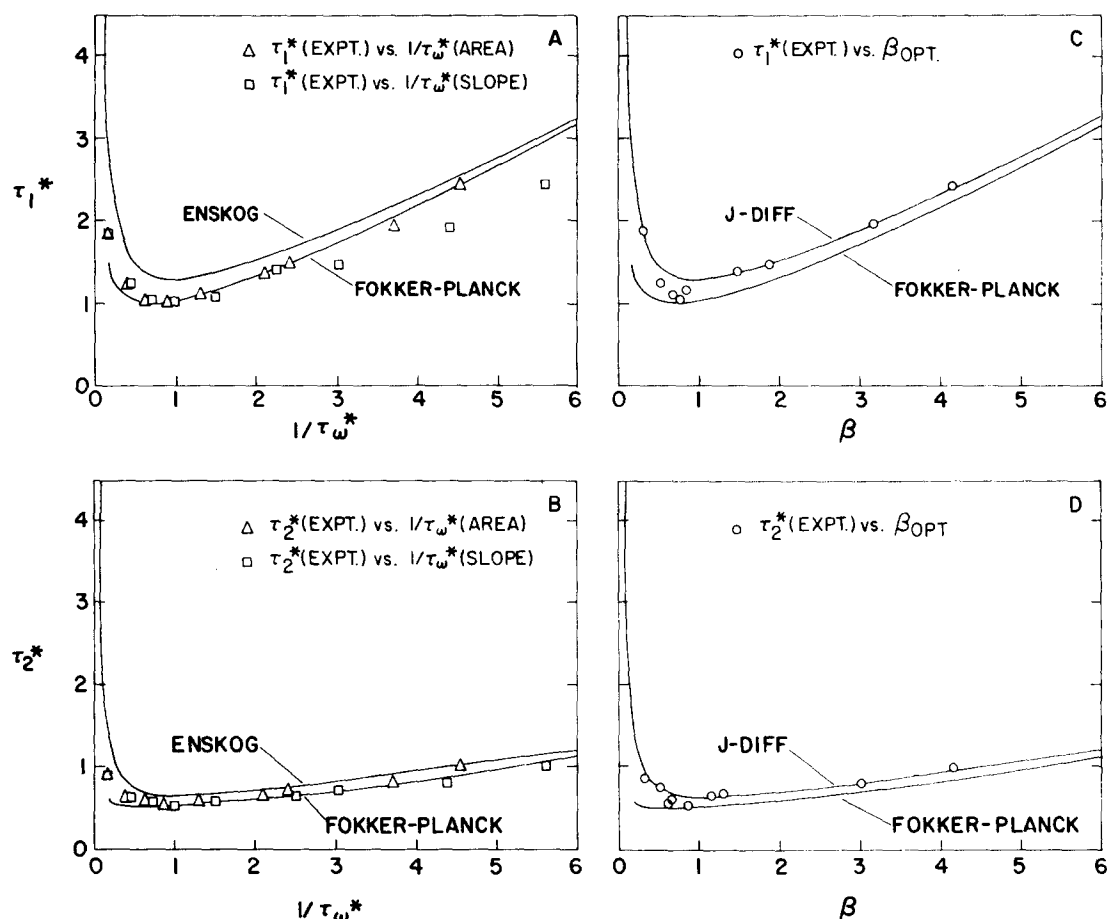FIG. 1. The orientational correlation times τ_1^* and τ_2^* [cf. Eq. (2.12)] are plotted vs $1/\tau w^*$ or β where τw^* is the angular velocity correlation time and β is an adjustable parameter that is defined in the text [cf. Eq. (1.1a)]. (A) The Enskog theory [cf. Eq. (3.19)] gives a theoretical prediction of τ_1^* vs $1/\tau_\omega^*$ (slope) which is indicated for τ_1^* by the upper curve. The Fokker–Planck theory gives a theoretical prediction for τ_1^* vs $1/\tau_\omega^*$(area) which is indicated for τ_1^* by the lower curve. The triangles ($\triangle\triangle\triangle$) indicate a plot of τ_1^* (exptl) vs $1/\tau_\omega^*$ (area), and the squares indicate a plot of τ_1^* (exptl) vs $1/\tau_\omega^*$ (slope). From this it would appear that the Fokker–Planck theory is consonant with experiment. (B) Same as (A), only for τ_2^*. (C) The upper curve represents the theoretical dependence of τ_1^* on the parameter β in the J-diffusion model, whereas the lower curve represents the theoretical dependence of τ_1^* on the reduced friction constant in the Fokker–Planck model. The open circles (o o o) indicate a plot of τ_1^* (exptl) vs β_{opt} where β_{opt} is determined by the prodedure given in connection with Eq. (2.14). Note that the experimental correlation times lie below the theoretical prediction in the neighborhood of the minimum. (D) Same as (C), only for τ_2^*.

In arbitrary fluids there is no well defined collision time and hence no independent way to determine the parameter β. Thus, one way to proceed is to determine τ_1^*(exptl) by calculating the area under an experimentally determined correlation function $C_l^{exptl}(\tau)$. Then β is found from theoretical curves like Fig. 1 by determining where τ_1^*(exptl) intersects the curve. For all values of τ_1^*(exptl) above the minimum value of τ_1^* allowed by the theory, there will be two possible values of β—that is, two roots. Only one of these roots is valid. The valid root is that one which, when used in conjunction with Eq. (2.8b), gives upon numerical Laplace inversion a correlation function $C_l(\tau)$ in closest agreement with the experimental function $C_l^{exptl}(\tau)$. Thus, if the theory is valid, we expect that corresponding to every experimental determination of $C_l(\tau)$ there will be a value of β. Now it is very important to recognize that if τ_1^*(exptl) is significantly less than the minimum in Fig. 1, there will be no value of β consistent with the experiment, and we must conclude that the J-diffusion model must be in-

valid. *Later we shall see that the correlation functions $C_l(\tau)$ determined from molecular dynamics studies of rough sphere fluids at certain densities are such that $\tau_1^*(exptl)$ is indeed significantly smaller than the minimum τ_1^*, thus indicating that the J-diffusion model cannot represent these fluids over the whole region of densities.*

Another obvious test is to measure $C_l(\tau)$ for two different values of l, say $l = 1$ and $l = 2$. *If these measurements are such that the resulting $\beta's$ are different for $C_1(\tau)$ and $C_2(\tau)$ determined for the same thermodynamic state, then clearly the Gordon model must be invalid.* This is another criterion of validity used in this paper.

It often happens that the experimental data $\{C_l(\tau)\}$ become progressively less accurate as τ increases or is not extensive enough to determine accurate values of τ_l^*. This is often the case in molecular dynamics. In this eventuality, we have designed the following procedure. The quantity $\Delta_l(T|\beta)$ is defined such that
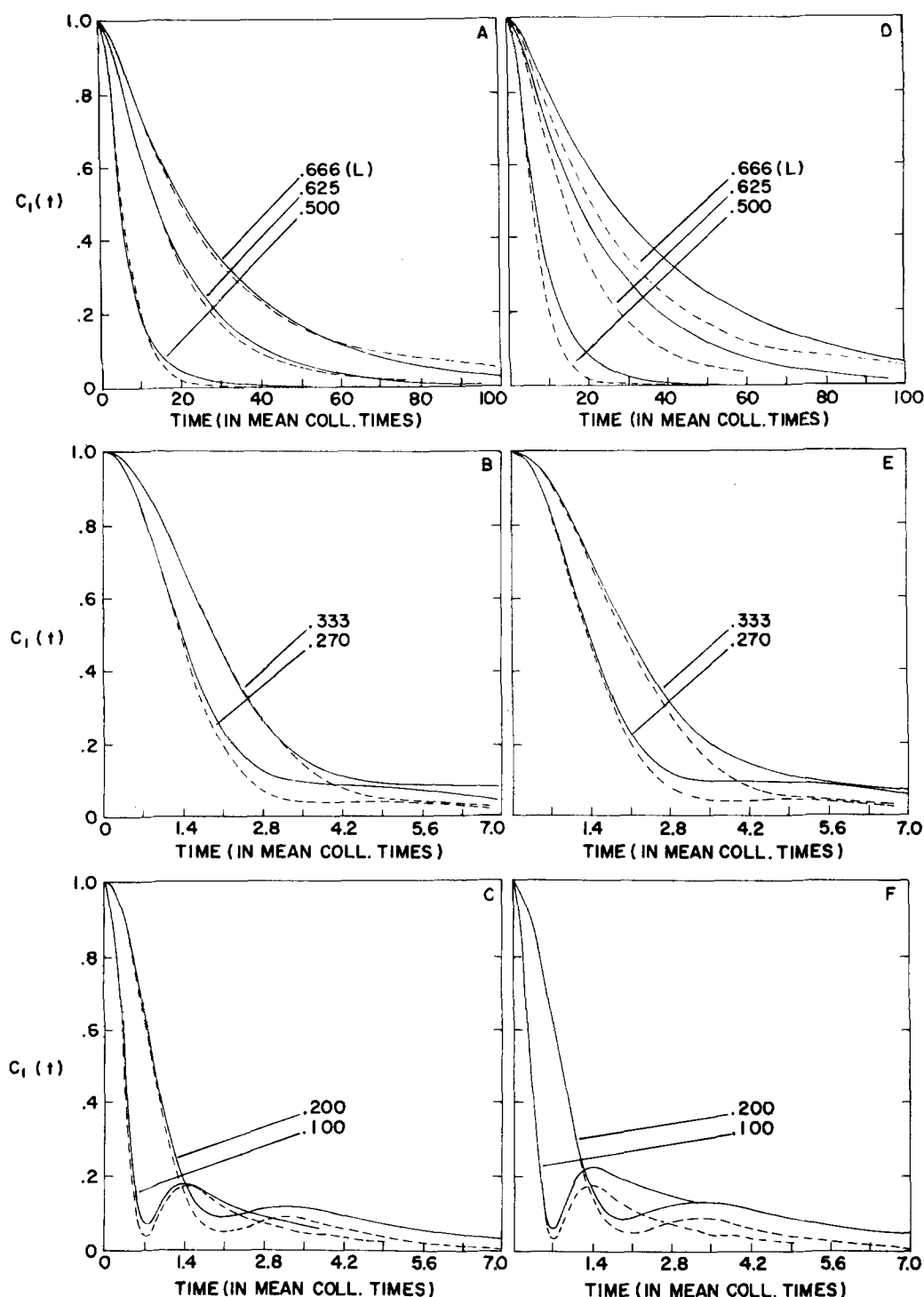
FIG. 2. A plot of the orientational correlation functions $C_1(\tau)$ vs the time in units of the collision time for various densities. In all the figures, the dashed lines are the dynamics data. In curves A, B, and C, the solid lines are the optimized J-diffusion results, and in D, E, and F, the solid lines represent the Enskog model. The densities are indicated with 0.666(l) denoting the liquid state at the highest density studied.

$$\Delta_i^2(\tau \mid \beta) \equiv \frac{1}{T} \int_0^T d\tau \, [C_i^{\text{expt1}}(\tau) - C_i(\tau; \beta)]^2 , \qquad (2.14)$$

where the cutoff T is chosen to include a good part of the decay. This quantity measures the deviation of the experimental function $C_i^{\text{expt1}}(\tau)$ from the theoretical function $C(\tau; \beta)$ for a given value of β. $\Delta_i(T \mid \beta)$ is computed as a function of β, and that β which minimizes $\Delta_i(T \mid \beta)$ is considered the optimum β. As we shall see, when the

data are extensive, these two methods give the same β; however, when the data are incomplete, this procedure is advantageous. The method adopted here is to use the area method where possible to guess a value of β and then to evaluate $\Delta_i(T \mid \beta)$ for a mesh of β's around this. The value of β that then minimizes Δ_i is then chosen as the optimum value of β.

Although we have discussed only the J-diffusion model

in detail, the same approach can be used for the M-diffusion model.

For sufficiently large β, Eq. (2.13d) should apply. It is not very difficult to show that in this limit inertial behavior quickly dies out and the correlation functions quickly become

$$C_l(\tau) \cong \exp - l(l+1)\beta^{-1}\tau \qquad (2.15a)$$

or

$$C_l(\tau) \cong \exp - \tau/\tau_l^* , \qquad (2.15b)$$

which follows from Eq. (2.10a). Thus, in the limit of high β, the Gordon model gives a simple exponential decay. The extended diffusion model has enjoyed considerable popularity. It is very physical and simple to apply. Moreover, it reduces to the Debye model for high densities. Unfortunately, we shall see that this is impossible to achieve at any stable fluid density. Chandler has developed an approximation scheme whereby β can be computed in the binary collision approximation. More shall be said about this in Sec. III.

C. Small step diffusion–the Debye model

Of the many theories of rotational relaxation, the oldest and best known is the Debye theory of rotational diffusion.[8] In this theory, the unit vector is assumed to perform a random walk on the surface of a unit sphere, consisting of infinitesimal angular steps. The resulting correlation functions have the form $C_l(t) = e^{-l(l+1)D_R t}$, where D_R is the rotational diffusion coefficient and t is the real time. Comparison with Eq. (2.15) shows that the Debye model is the high β limit of the Gordon model, and gives D_R in terms of β,

$$D_R = \left(\frac{kT}{I}\right)^{1/2}\beta^{-1} . \qquad (2.16)$$

D. The jump diffusion model

Another model, first put forward by Ivanov,[9] is the jump diffusion model in which u performs a random walk on the surface of unit sphere that is not restricted to infinitesimal angular jumps. This theory results in

$$C_l(\tau) = \exp - t/\tau_l^0, \qquad (2.17a)$$

where

$$\frac{1}{\tau_l^0} \equiv \frac{[1 - \langle P_l(\cos\theta)\rangle]}{\tau_j} \frac{1}{\tau_j} , \qquad (2.17b)$$

where τ_j is the mean time between jumps, θ is the jump angle, and $\langle \ldots \rangle$ denotes an average over the jump angle distribution function. This reduces to the result of the Debye model if only very small angular jumps are made for then $1/\tau_l^0 = l(l+1)D_R$, where $D_R = \langle\theta^2\rangle/4\tau_j$. This model is not terribly relevant to our studies.

E. The Fokker–Planck model

The angular momentum of a molecule can be regarded as a Gaussian stochastic process and can thus be described by a Langevin equation

$$\frac{d\omega_i}{dt} = \Gamma_i \omega_j \omega_k - \gamma_i \omega_i + A_i(t) , \qquad (2.18a)$$

where ω_i is the ith componentent of the angular velocity, γ_i is a friction constant, A_i is related to the random torque, and $\Gamma_i = (I_j - I_k)/I_i$, where I_i is the moment of inertia about a body fixed axis. For a rough sphere $I_i = I_j = I_k = I$, and $\gamma_i = \gamma_j = \gamma_k = \gamma$, so that the Langevin equation simplifies to

$$d\omega/dt = -\gamma\omega + A(t) . \qquad (2.18b)$$

If the random torque is assumed to be a Gaussian random process, as is usually the case in Brownian motion theory, the Langevin equation can be used to derive the Fokker–Planck equation[13]

$$\left[\frac{\partial}{\partial t} + i\omega \cdot \hat{\mathbf{I}} - \gamma\nabla_\omega \cdot \left(\nabla_\omega + \left(\frac{I}{kT}\right)\omega\right)\right] P(\omega, \mathbf{u}, t; \omega_0, \mathbf{u}_0, 0) = 0 , \qquad (2.19a)$$

where $P(\omega, \mathbf{u}, t; \omega_0, \mathbf{u}_0, 0)$ is the joint probability distribution for finding a particle with orientation $\mathbf{u}_0$, angular velocity ω_0 at time $t = 0$ and with orientation $\mathbf{u}$, angular velocity ω at time t. The operator $\hat{\mathbf{I}}$ is the dimensionless angular momentum operator of quantum mechanics, and the term $i\omega \cdot \hat{\mathbf{I}}$ generates the free particle rotation. The differential operator which appears as a factor of γ represents the collisional relaxation. Equation (2.18b) must be solved subject to the boundary conditions

$$P(\omega, \mathbf{u}, 0; \omega_0, \mathbf{u}_0, 0) = P_{eq}(\omega)\, \delta(\omega - \omega_0)\, \delta(\mathbf{u} - u_0) , \qquad (2.19b)$$

where $P_{eq}(\omega_0)$ is the Maxwell distribution function. With the solution of Eqs. (2.19), the correlation functions can be determined. For example,

$$\begin{pmatrix} C_l(t) \\ C_\omega(t) \end{pmatrix} = \int d\omega \int d\omega_0 \int d\mathbf{u} \int d\mathbf{u}_0$$

$$\times \begin{pmatrix} P_l(\mathbf{u} \cdot \mathbf{u}_0) \\ \omega \cdot \omega_0 \end{pmatrix} P(\omega, \mathbf{u}, t; \omega_0, \mathbf{u}_0, 0) . \quad (2.20)$$

It is useful to express the time in reduced units $\tau = (kT/I)^{1/2}t$ and the friction constant in reduced units $\beta = \gamma(I/kT)^{1/2}$. In these units,

$$C_\omega(\tau) = e^{-\beta\tau} , \qquad (2.21a)$$

so that the angular velocity correlation time τ_ω^* in these reduced units is

$$1/\tau_\omega^* = \beta . \qquad (2.21b)$$

$C_\omega(t)$ is relatively easy to evaluate, since it follows directly from the Langevin equation. The solution of Eqs. (2.19) $C_l(\tau)$ is much more difficult, and in fact, no analytical solution has yet been given in three dimensions. Nevertheless, Fixman and Rider[12,17] have numerically solved Eqs. (2.19) and (2.20) and have determined $C_l^{(F-P)}(\tau)$ for different parameter β. We shall subsequently compare the molecular dynamics with this numerical solution.

III. THE ROUGH SPHERE FLUID

In fluids composed of molecules that interact through continuous potentials, there is no uniquely defined collision time because each molecule may be in continuous interaction with its neighbors. In contrast, fluids containing "hard particles" have uniquely defined collision times. The mean time between successive collisions[18]

t_c experienced by a rough sphere of diameter σ is given by

$$\frac{1}{t_c} = 4\pi\sigma^2 \rho g(\sigma)\left(\frac{kT}{\pi m}\right)^{1/2} , \qquad (3.1)$$

where ρ is the number density, $g(\sigma)$ is the contact pair correlation function, and t_c is given in seconds. It is common in the literature to use the Enskog time t_E, where

$$1/t_E \equiv \tfrac{2}{3}(1/t_c) .$$

Combining Eqs. (1.1) and (3.1) then gives an *a priori* calculation of β,

$$\beta_c = \sqrt{8\pi\kappa}\,\hat{\rho}g(\sigma) = \frac{1}{\tau_c} , \qquad (3.2)$$

where c denotes that β has been computed using t_c, τ_c is the collision time in reduced units, and

$$\hat{\rho} \equiv \rho/\rho_{c.p.} = (\rho\sigma^3)/\sqrt{2} , \qquad (3.3a)$$

$$\kappa \equiv 4I/m\sigma^2 . \qquad (3.3b)$$

Here I is the moment of inertia of the rough sphere, and $\rho_{c.p.}$ is the density of the rough sphere system when it is *closest packed* ($\rho_{c.p.} = \sqrt{2}/\sigma^3$). $\hat{\rho}$ is simply the number density expressed in units of the density at closest packing. For future reference it is important to note that the rough sphere fluid exhibits a liquid–solid phase transition at $\hat{\rho} = 2/3$. The parameter κ measures the mass distribution within a sphere. If the mass is localized at the center of the sphere $\kappa = 0$, if it is distributed uniformly over the sphere $\kappa = 2/5$, and if it is concentrated on the surface of the sphere, κ reaches a maximum of $\kappa = 2/3$. As κ increases from $\kappa = 0$ to $2/3$, the flywheel capacity of the sphere increases.

According to Eq. (3.2), β_c does not depend on the temperature, but does depend on $\hat{\rho}$—both directly and through the dependence of $g(\sigma)$ on $\hat{\rho}$. An excellent approximation for $g(\sigma)$ in the fluid state is[19]

$$g(\sigma) = \frac{(2 - \eta)}{2(1 - \eta)^3} , \qquad (3.4a)$$

where

$$\eta \equiv \frac{\sqrt{2}\pi}{6}\,\hat{\rho} . \qquad (3.4b)$$

The dependence of β_c on $\hat{\rho}$ is thus easily found by combining Eq. (3.2) with Eq. (3.4).

Although the initial formulation of the Gordon model requires that the parameter in Eq. (2.6) should be β_c, it will be shown that this results in a paradox, and a contradictory result. This question will be dealt with later.

The collision dynamics in a rough sphere fluid are completely defined[7] by the laws of conservation of linear and angular momentum and the following law of interaction between two spheres, labeled 1 and 2. A collision between 1 and 2 causes a complete reversal of the relative tangential velocity $\mathbf{g}_{21}$ of the colliding pair where

$$\mathbf{g}_{21} = \mathbf{v}_{21} + \tfrac{1}{2}\sigma\mathbf{n} \times (\omega_1 + \omega_2) \qquad (3.5)$$

and where ω_i and $\mathbf{v}_i$ are the angular velocity and the

center of mass linear velocity of particle i, $\mathbf{v}_{21} = \mathbf{v}_2 - \mathbf{v}_1$ is the relative center of mass velocity of particle 2 with respect to particle 1, and $\mathbf{n}$ is a unit vector pointing along the line of centers from 1 to 2 when the particles are colliding (kissing). Since $\mathbf{g}_{21}$ is completely reversed by the collision, the relative tangential velocity $\mathbf{g}'_{21}$ after the collision is simply $\mathbf{g}'_{21} = -\mathbf{g}_{21}$. In the following, a primed quantity will always denote a quantity after a collision and an unprimed quantity will always denote that property before a collision. From this it follows (see Chapman and Cowling)[7] that

$$\mathbf{v}'_1 = \mathbf{v}_1 + \frac{\kappa}{\kappa + 1}\left[\mathbf{v}_{21} + \frac{\sigma}{2}\mathbf{n}\times(\omega_1 + \omega_2) + \frac{1}{\kappa}\,\mathbf{n}\mathbf{n}\cdot\mathbf{v}_{21}\right] , \qquad (3.6a)$$

$$\omega'_1 = \omega_1 + \left[\frac{\sigma}{2}\,(\kappa + 1)\right]^{-1}\left\{\mathbf{n}\times\left[\mathbf{v}_{21} + \frac{\sigma}{2}\mathbf{n}\times(\omega_1 + \omega_2)\right]\right\} , \qquad (3.6b)$$

with similar expressions for $\mathbf{v}'_2$ and ω'_2. These equations essentially define the rough sphere interaction.

Our objective is to determine among other things the time autocorrelation functions[20] of the properties $\mathbf{v}_1$ and ω_1. These functions have the form

$$C_A(t) = \frac{\langle A_1 e^{iLt} A_1\rangle}{\langle |A_1|^2\rangle} , \qquad (3.7a)$$

where A_1 is either $\mathbf{v}_1$ or ω_1, the bracket $\langle\ \rangle$ indicates an average over the canonical ensemble, and L is the Liouville operator.[20] Equation (3.7a) can be expressed as

$$C_A(t) = \langle\langle e^{iLt}\rangle\rangle_A , \qquad (3.7b)$$

where $\langle\langle \cdots \rangle\rangle = \langle A_1(\cdots)A_1\rangle \cdot \langle A_1 A_1\rangle^{-1}$ defines a new average, and $C_A(t)$ is the average value of the propagator. Equation (3.7b) can be expressed as a cumulant expansion[21]

$$C_A(t) = \exp\sum_{n=1}^{\infty} \frac{\kappa_n t^n}{n!} , \qquad (3.8a)$$

where for example

$$\kappa_1 = -\frac{1}{t_A} = \langle\langle iL\rangle\rangle_A , \qquad (3.8b)$$

$$\kappa_2 \equiv \langle\langle (iL)^2\rangle\rangle_A - [\langle\langle iL\rangle\rangle_A]^2 . \qquad (3.8c)$$

This kind of approximation was recently exploited by Chandler.[22] If the cumulant expansion is truncated after the first term, one finds that

$$C_A(t) = \exp - t/t_A , \qquad (3.9)$$

where $1/t_A$ is given by Eq. (3.8b). Chandler asserts[23] that truncation at this level is equivalent to assuming that only sequences of uncorrelated binary collisions contribute to $C_A(t)$. *Any deviation from Eq. (3.9) therefore must arise from correlated binary collisions.*

In order to proceed, it is necessary to evaluate the correlation time t_A which is defined by Eq. (3.8b) explicitly by

$$\frac{1}{t_A} = \frac{\langle A_1 iLA_1\rangle}{\langle A_1^2\rangle} . \qquad (3.10)$$

Now the Liouville operator in a hard sphere system can be expressed as[24]

$$iL = iL_0 - \sum_{j > i = 1} T_{ji} \, ,$$

where L_0 is the free particle Liouville operator and T_{ji} is the binary collision operator for the pair of particles (i, j) defined by Zwanzig.[24] If the quantity A_1 does not depend on the position (like v_1 or ω_1), then $iL_0 A_1 = 0$ and $iLA_1 = -\sum_{j > i} T_{ji} A_1$. Clearly, collisions between $i \neq 1$ and $j \neq 1$ do not change A_1, so that $iLA_1 = -\sum_{j > 1} T_{j1} A_1$ and Eq. (3.10) becomes[22]

$$\frac{1}{t_A} = - \frac{\langle A_1 \sum_{j > 1} T_{j1} A_1 \rangle}{\langle A_1^2 \rangle} = - (N - 1) \frac{\langle A_1 T_{21} A_1 \rangle}{\langle A_1^2 \rangle} \, , \quad (3.11)$$

where in the last equality recognition was taken of the fact that all T_{j1} $(j = 2, \ldots, N)$ give the same result.

Zwanzig[24] has provided a method for determining averages like Eq. (3.11). By generalizing the derivation of Zwanzig's Eq. (A13) (Ref. 24) to take into account excluded volume effects, it follows that for rough spheres of diameter σ,

$$\frac{1}{t_A} = \langle A_1^2 \rangle^{-1} \rho g(\sigma) \left\langle \int_0^{2\pi} d\phi \int_0^{\sigma} db\, b \, |v_{21}| \, A_1 [A_1' - A_1] \right\rangle \, , \quad (3.12)$$

where A_1 and A_1' are the properties of A_1 before and after a collision of particle 1 with particle 2 with impact variables (b, ϕ) and COM relative velocity v_{21}. The brackets indicate an average over the Maxwellian distribution of particles 1 and 2. In order to evaluate this integral, A_1' must be calculated using Eqs. (3.6a) and (3.6b). Then for v_1 and ω_1, the well known results (see, for example, Ref. 22 and references cited therein),

$$\frac{1}{t_v} = \frac{2}{3} \left(\frac{2\kappa + 1}{\kappa + 1} \right) \frac{1}{t_c} \, , \quad (3.13a)$$

$$\frac{1}{t_\omega} = \frac{2}{3(\kappa + 1)} \frac{1}{t_c} \quad (3.13b)$$

are obtained, where t_c is given by Eq. (3.1) and κ is defined by Eq. (3.3b). Thus, if one can ignore correlated binary collisions, the velocity and angular velocity correlation functions are

$$C_v(t) = e^{-|t|/t_v} \, , \quad (3.14a)$$

$$C_\omega(t) = e^{-|t|/t_\omega} \, . \quad (3.14b)$$

These are often called *Enskog correlation functions* because in their derivation, as in the derivation of the Enskog equation (of the kinetic theory of dense fluids), *correlated binary collisions* (c. b. c.) *are ignored*. Deviations from these functions therefore measure the importance of correlated binary collisions.

Return for a moment to the Gordon theory of extended diffusion.[8] In that theory it is assumed (a) that successive collisions are uncorrelated, and moreover (b) that each collision randomizes the angular velocity. From (a) it follows that the collision times are distributed according to a Poisson distribution; that is,

$$P_n(t) = \frac{1}{n!} \left(\frac{t}{t_c} \right)^n e^{-t/t_c} \, , \quad (3.15)$$

where $P_n(t)$ is the probability that a particle will experience n collisions in the time t, where t_c is the mean free time. Now in computing $C_\omega(t)$ it follows from (b) that

since there is no correlation between the angular velocity before and after a collision, $C_\omega(t)$ must be equal to the fraction of particles that have not yet collided in the time t or $P_0(t)$. From Eq. (3.15) it then follows that

$$C_\omega^{(G)}(t) = e^{-|t|/t_c} \, , \quad (3.16)$$

where the superscript G indicates that this result springs from a quite literal interpretation of the Gordon model. The important thing to note is that the Gordon model is much more restrictive than the independent binary collision (I. B. C.) model. Since $t_c < t_\omega$, the Gordon model predicts a shorter correlation time for $C_\omega(t)$ than does the I. B. C. model. Thus, if we use Eq. (3.16) together with Eq. (2.8b), we will obtain $C_l^{(G)}(t)$, which corresponds to a too rapidly decaying angular velocity. In point of fact, Eq. (3.16) cannot describe the dynamics of any real fluid because it does not satisfy the moment theorems, whereas Eq. (3.14b) may be a reasonable approximation. Comparisons of this sort are made in Sec. IV.

Thus, if the Gordon model is taken seriously, a contradiction results. In the Gordon theory the primary event is a collision, and it is assumed that this event randomizes the angular velocity. This latter assumption is clearly in error. It is possible, however, to salvage the extended diffusion model by assuming that there are independent events—albeit fictitious events—separated on the average by the time t_ω (not t_c) and such that the angular velocity is randomized after each such event. This model gives Eq. (3.14b) and, moreover, gives Eq. (2.8b) if we take β equal to

$$\beta_\omega = (I/kT)^{1/2} \frac{1}{t_\omega} = \frac{2}{3(\kappa + 1)} \beta_c = \frac{1}{\tau_\omega^*} \, , \quad (3.17)$$

where the next to last equality follows from Eqs. (3.13b) and (3.2), and τ_ω^* is t_ω in reduced units.

This attempt to salvage the model is somewhat artificial. Chandler[11] has, however, developed a simple scheme similar to that which led to Eq. (3.9). Chandler first writes down the cumulant expansion of the memory function $K_l(t)$ corresponding to $C_l(t)$. He then writes

$$K_l(t) = K_l^{(0)}(t) \exp \sum_{n=1}^{\infty} (\kappa_n - \kappa_n^{(0)}) \frac{t^n}{n!} \, , \quad (3.18a)$$

where $K_l^{(0)}$ is the memory function of a system of free rotors, and $\kappa_n^{(0)}$ are the cumulants of the free rotor system. Chandler then asserts that a truncation of the cumulant expansion after $n = 1$ is equivalent to an approximation in which only sequences of uncorrelated binary collisions are kept. This is the same approximation which leads to Eq. (3.14b). He then shows that $(K_1 - K_1^{(0)}) = -1/t_\omega$, so that the I. B. C. approximation gives

$$K_l^{(ENSK)}(t) = K_l^{(0)}(t) e^{-t/t_\omega} \, , \quad (3.18b)$$

where the superscript ENSK refers to the independent binary collision (or ENSKOG) model. This approximation will be referred to in the sections as the Enskog approximation, and the correlation functions springing from this approximation will be denoted by a super-

script (ENSK). As far as we know, this may well be the first attempt to place the J-diffusion model on a molecular basis.

The memory function equation for $C_l(t)$ then takes the form

$$\tilde{C}_l^{(ENSK)}(s) = \frac{1}{s + \tilde{K}_l^{(0)}(s + 1/t_\omega)} \quad,$$

where from Eq. (3.18) we have used $\tilde{K}_l(s) = \tilde{K}_l^{(0)}(s + 1/t_\omega)$. Now clearly, $\tilde{C}_l^{(0)}(s) = (s + \tilde{K}_l^{(0)}(s))^{-1}$. Eliminating $\tilde{K}_l^{(0)}(s + 1/t_\omega)$ in favor of $\tilde{C}_l^{(0)}(s + 1/t_\omega)$ gives, in reduced units,

$$\tilde{C}_l^{(ENSK)}(P) = \frac{\tilde{C}_l(P + \beta\omega)}{1 - \beta_\omega \tilde{C}_l(P + \beta_\omega)} \quad, \tag{3.19}$$

where $p = s(I/kT)^{1/2}$, and $\beta_\omega = (I/kT)^{1/2}t_\omega^{-1}$ are in the reduced units used throughout this paper. This is the same result obtained from the J-diffusion model [Eq. (2.8a)] by substituting t_ω in place of t_c. The very nice thing about the I. B. C. model is that it is internally consistent. Nevertheless, its validity must be tested against molecular dynamics. What is remarkable is that this very plausible model does not agree with experiment throughout the whole density regime.

It should be noted that of the Enskog model[11] were valid, it would give upon combining Eqs. (3.17), (2.13), and (2.16),

$$\tau_l^* = (1/2l)\tau_\omega^* \quad \text{(dilute fluid)}, \tag{3.20a}$$

$$\tau_l^*\tau_\omega^* = 1/l(l+1) \quad \text{(dense fluid)}, \tag{3.20b}$$

$$D_R^* = \tau_\omega^* = 1/\beta \quad \text{(dense fluid)}, \tag{3.20c}$$

where $\tau_\omega^* = (kT/I)^{1/2}t_\omega$ is the angular velocity correlation time in reduced units and D_R^* is the rotational diffusion coefficient in reduced units. These equations are variants of the Hubbard relations which have been derived in several different ways. The importance of these relations is that they give a relationship between the orientational correlation time and the angular velocity correlation time. At low densities τ_l^* is proportional to τ_ω^* because the area under $C_l(\tau)$ decreases as collision reorient the angular velocity and thereby destroy the projection of u on the initial value of $\omega(0)$. At high densities, τ_l^* is inversely proportional to τ_l^* because rapid changes in ω lead to smaller step diffusion of u. The original relation derived by Hubbard[14] was for high densities and is analogous to Eq. (3.20b),

$$\tau_l^*\tau_\omega^*(\text{area}) = 1/l(l+1) \quad, \tag{3.21}$$

where $\tau_\omega^*(\text{area})$ is the area under $C_\omega(\tau)$. Hubbard did not discuss the low density limit.

IV. EXPERIMENTAL METHOD

In order to test the foregoing models of rotational relaxation, molecular dynamics calculations were performed on rough sphere fluids at the ten densities, $\hat{\rho} = 0.01$, 0.1, 0.2, 0.27, 0.3, 0.333, 0.4, 0.555, 0.625, and 0.666. Although the basic procedure is quite similar to that used to study smooth sphere fluids, there are significant differences that arise owing to the presence of the rotational degrees of freedom.

In molecular dynamics a system of N rough spheres in a box of volume V is simulated by solving the equations of motion subject to periodic boundary conditions. The phase space trajectory generated is then used to determine the time dependence of various dynamical properties and correspondingly, through time averaging, both static properties and time correlation functions.[3,20]

These are several important parts of a molecular dynamics study. First, one must choose the initial conditions. Second, one must develop an algorithm for solving the equations of motion. Third, one must decide on criteria for bringing the system to "equilibrium." Finally, one must develop efficient codes for determining the static properties and time correlation functions. The remainder of the section is devoted to an explanation of some of the details involved in our procedure.

A. Part I: Initial conditions

The initial state is so chosen that the total linear and angular momentum of the N particle system is zero. This is accomplished by sampling the linear and angular momenta of $N-1$ of the molecules from a Maxwell–Boltzmann distribution. The remaining particle is assigned a linear and angular momentum such that the total linear and angular momentum is zero.

The initial configuration of the system is so chosen that the centers of the N spheres are placed on the points of a face centered cubic (fcc) lattice of appropriate dimensions for the density under study. This limits the study to systems containing 4, 32, 108, 256, ... spheres. This initial solid configuration is obviously far removed from the typical configuration of a liquid. As the dynamics code runs the spheres leave their lattice positions and eventually, after many collisions, occupy a configuration which is typical of the liquid state. Several criteria are used to determine when this has occurred. These are described later. The system is then said to be *equilibrated*.

An alternative procedure would be to sample the configuration using well developed Monte Carlo codes. Another procedure is to scale the positions of a previously equilibrated dynamics run.

At the density $\hat{\rho} = 0.6666$ there is a solid to liquid phase transition.[3] Starting out in the fcc configuration, it was found that a very large number of collisions is necessary before melting takes place. Thus, it is easy to study the ordered phase at this density. On the other hand, it is very inefficient to wait for the system to spontaneously disorder. Thus, the initial states of the disordered phase at $\hat{\rho} = 0.6666$ were generated from an equilibrated trajectory of the fluid at $\hat{\rho} = 0.625$ by expanding the volume of the spheres at each collision, taking care that no two spheres overlapped. This was done until a density of 0.6666 was reached.

All of this work is done in the reduced units in which the molecular mass is one, the molecular radius is one, and the linear velocities are scaled to give $k_B T = 1$. In these units the moment of inertia of the spheres can vary from 0 to 2/3. In particular, when the mass is entirely concentrated in the center, $I = 0$. When the

mass is distributed uniformly over the sphere, $I = 2/5$, and when the mass is concentrated on the surface of the sphere, $I = 2/3$. The value of I in these reduced units is simply κ given in Eq. (3.3b). In these units the velocities are measured in units of $(k_B T/M)^{1/2}$ and the Maxwell distribution is $(2\pi)^{-3/2} e^{-v^2/2}$. The properties of the rough sphere fluid, like those of the smooth sphere system, when expressed in reduced units, do not depend explicitly on the temperature. In fact, the only significant parameters for the specification of the state are the density $\hat{\rho}$ and the mass distribution parameter κ.

B. Part II: Trajectory calculations

The studies reported here involve a small number of molecules ($N = 108$) in a box of volume V. The motions of these molecules are solved subject to periodic boundary conditions. The system can thus be regarded as an infinite system consisting of the "real particles" in the original box and their periodic "image particles." Thus, if a real particle i has position (x_i, y_i, z_i), it has images at $x_i + L$, $x_i + 2L$, etc. Not only collisions between two real particles but collisions between a real particle and image particles must be considered in the calculation of the phase trajectory.

In hard sphere fluids the particles follow linear trajectories between instantaneous collisions. The first step is to examine all pairs of molecules and to determine for which pair there will be a collision. If there is a collision, the time at which it occurs is stored in a list and a pointer is attached to the collision pair. This list is easily constructed from the known positions and velocities of the particles. The list is now examined to determine the shortest collision time T_s and thereby the pair of particles that will collide first. The time T_s is subtracted from the other times listed and the molecules are all advanced along free particle trajectories for the time T_s. The linear and angular velocities of the colliding pair are then changed according to Eq. (3.6). The time at which the collision occurred and the new linear and angular velocities are stored on disc. The two collision partners are then examined with respect to all the other molecules and their images to find out if the previously constructed list of collision times should be changed.

This procedure is repeated. The total energy, linear momentum, and angular momentum are checked periodically to ascertain whether the algorithm is of sufficient accuracy to satisfy the laws of conservation of total energy, linear momentum, and angular momentum. When the desired number of collisions is reached, the final total phase point is stored for future enlargement of the trajectory. Needless to say, the information stored on disc allows reconstruction of the full phase space trajectory whenever it is needed. The storage required for 10 800 collisions is 2.1×10^6 bytes of direct access storage, 1.7×10^5 bytes of core storage, and approximately 20 min of CPU time on an IBM 360/91 computer.

C. Part III: Equilibration

A suitable measure of the translational order in the system is given by the translational order parameter

$$\zeta(t) = \frac{1}{3} \sum_{j=1}^{N} \left[\cos kx_j(t) + \cos ky_j(t) + \cos kz_j(t) \right], \quad (4.1)$$

where $k = 4\pi/s$ and where s is the distance along the x axis between the molecules on the fact of the fcc lattice at the density under study. Given our choice of initial conditions, $\zeta(0) = N$. If the system disorders, $\zeta(t)$ should decay from its initial value N and after a sufficient time should fluctuate around an average value of zero. The amplitude of these fluctuations should be $\pm \sqrt{N}$. In this latter region, the fluid is said to be in "configurational equilibrium." If the system remains in the solid phase, $\zeta(t)$ should decay to some nonzero value about which it should continue to fluctuate. It is then said to be in configurational equilibrium. At the highest density studied ($\hat{\rho} = 0.6666$), we were able to equilibrate at two different order parameters: one finite ($\zeta \sim 108$, solid) and one zero ($\zeta = 0$, fluid). For all lower densities the equilibrium configuration corresponded to $\zeta = 0$ (fluids).

In addition to the order parameter ζ, the pressure P and the contact pair correlation function $g(\sigma)$ were calculated using the virial theorem as outlined by Wood.

When both $\zeta(t)$ and $g(\sigma)$ fluctuate by no more than 5% around their respective average values, the system is assumed to be in equilibrium. A trajectory consisting of 10 800 collisions is then computed for this system in microcanonical equilibrium.

D. Part IV: Time correlation functions

The time correlation function of the property A can be evaluated as follows. The time over which the trajectory is known, T, is divided into M equally spaced time intervals Δt ($T = M\Delta t$). Denoting A_j and A_{j+n} the values of the property A at time $t_j = j\Delta t$ and $t_{j+n} = (j + n)\Delta t$, it is clear that the time correlation function of A can be expressed as

$$\langle A(0) A(t_n) \rangle = \frac{1}{M-n} \sum_{j=1}^{M-n} A_j A_{j+n} . \quad (4.2)$$

If Δt is chosen very small compared to the correlation time of the function, there will be much unnecessary and time consuming calculation, whereas if Δt is chosen to be of the order of the correlation time, the resulting function might be greatly in error. The choice of Δt, often called the *graining*, is totally within our control.

In the case of single particle properties, $A^{(\alpha)}$ is the property of the αth molecule and Eq. (4.2) takes the form

$$\langle A(0) A(t) \rangle = \frac{1}{N(M-n)} \sum_{\alpha=1}^{N} \sum_{j=1}^{M-n} A_j^{(\alpha)} A_{j+n}^{(\alpha)} . \quad (4.3)$$

The data written on the disc in Sec. IV. C are written at unevenly spaced time intervals. In order to utilize Eq. (4.3) for the calculation of $C_v(t)$ and $C_\omega(t)$, it is necessary to reformat these data in such a way that the phase space trajectory for the equilibrated system is written in equally spaced time intervals. In all of our

TABLE I. Initial slopes in mean collision times.

$\hat{\rho}$	$\dfrac{1}{\tau_v}$	$\dfrac{1}{\tau_\omega}$
0.100	0.862	0.457
0.200	0.862	0.477
0.270	0.877	0.465
0.333	0.857	0.473
0.400	0.857	0.475
0.500	0.857	0.477
0.555	0.885	0.466
0.625	0.835	0.459
0.666(l)	0.866	0.475
0.666(s)	0.861	0.472
Average	0.862	0.472
Theory	0.857	0.476

studies, the equilibrated trajectory contains 10 800 collisions, and the value of κ is 0.4, corresponding to a sphere of uniform mass distribution. The graining chosen is anywhere between 0.1 and 0.4 collisions per particle, depending on the correlation function and the density being studied. The program produces three randomly accessable files of data—one for the linear velocities, one for the angular velocities, and one containing information necessary for the calculation of $C_1(t)$ and $C_2(t)$.

Files for a 108 particle trajectory are stored on an STC Model 3330 Random Access Disc Drive and occupy approximately 900 tracks of 13 000 bytes each for latter processing. This program normally requires 10 min of execution time on an IBM 360/91.

In the early stages of this project, $C_1(t)$ and $C_2(t)$ were evaluated by assigning unit vectors $\mathbf{u}$ to each molecule in a random fashion and evaluating the correlation function by direct calculation of Eq. (4.3). Because the correlation functions are very sensitive to the relative orientation of $\mathbf{u}$ with respect to ω, this method was rejected because it was felt that it might introduce errors in the correlation functions.[25] An alternative procedure was therefore adopted. In this procedure, a set of three orthogonal body fixed axes are embedded rigidly in each sphere. The reorientation of the body fixed axes of the αth molecule is completely specified by the direction cosine matrix $\mathbf{R}^{(\alpha)}(t)$ evaluated in the laboratory fixed coordinate system. Given the information generated on Block 2, the matrix elements, $R_{ij}^{(\alpha)}(t)$, can be determined and stored on disc in equally spaced time increments. If $\mathbf{u}^{(\alpha)}$ is a unit vector rigidly embedded in the αth sphere, then

$$u_i^{(\alpha)}(t) = R_{ij}^{(\alpha)}(t)\, u_j^{(\alpha)}(0) , \qquad (4.4)$$

where the Einstein summation convention is implied; and where $u_i^{(\alpha)}(t)$ is the ith component of $\mathbf{u}^{(\alpha)}(t)$ in the laboratory fixed coordinate system at time t. Equation (4.4) can be used to evaluate the correlation function $C_1(t)$ and $C_2(t)$.

To accomplish this, it is important to note that

(a) in an isotropic ensemble $\langle u_i u_k\rangle = \tfrac{1}{3}\delta_{ik}$;

(b) $\mathbf{R}(t)$ is an orthogonal matrix, so that $R_{ij}(t) = R_{ji}^{-1}(t)$. Then it is easy to show that

$$C_1(t) = \tfrac{1}{3}\langle \mathrm{Tr}\mathbf{R}^{-1}(0)\cdot\mathbf{R}(t)\rangle \qquad (4.5a)$$

and

$$C_2(t) = \tfrac{1}{10}\left\{ \langle [\mathrm{Tr}\mathbf{K}(t)]^2\rangle - \langle \mathrm{Tr}\mathbf{K}(t)\cdot\mathbf{K}(t)\rangle - 2\right\} , \qquad (4.5b)$$

where

$$K(t) = \mathbf{R}^{-1}(t')\cdot\mathbf{R}(t'+\tau) . \qquad (4.5c)$$

These functions $C_l(t)$ are easily found from appropriate time averages of the rotation matrices.

V. DATA ANALYSIS

The initial slopes of $C_v(t)$ and $C_\omega(t)$ were evaluated by fitting polynomials of order 1–4 to the log of the first ten points of the correlation functions and choosing for the slope the value of the linear term of the polynomial which has the smallest variance. The error was estimated to be ~1% from the Zwanzig–Ailawadi formula and was estimated to be 3% on the basis of several trajectories run at a density of 0.3333. These initial slopes are tabulated in Table I, in units of the inverse mean collision time, along with the initial slope predicted theoretically using the binary collision operator [see Eq. (3.13)]. The agreement should be noted, since it is a measure of the consistency of the molecular dynamics study.

The velocity and angular velocity correlation times determined from the initial slope are called the *Enskog correlation times* in the ensuing discussion. In the literature, the correlation time of a random variable is defined as the area under its time correlation function [cf. Eq. (2.12)]. In the ensuing discussion, these correlation times are denoted by (area), and are evaluated by Simpson's rule integration of the experimental correlation functions. Table II contains both the velocity and angular velocity correlation times determined from the initial slope (Enskog) and from the area. These data are presented in reduced units—that is, in units of the free rotor tumbling time $(I/kT)^{1/2}$. Table II contains additional data—all in the above reduced units. τ_1^* and τ_2^* are the correlation times of $C_1(\tau)$ and $C_2(\tau)$, τ_c^* is the Enskog collision time, and β_1 and β_2 are the values of β which give, respectively, the best fits of the Gordon J-diffusion model[10] to the experimental $C_1(\tau)$ and $C_2(\tau)$. These values are called the optimized values of β. Equations (2.13a) and (2.13b) are used to determine the dependence of τ_1^* for the J-diffusion model on β. This is plotted in Fig. 1. For the sake of comparison, the experimental τ_1^* are plotted vs the optimized β_1 on the same curve. The poor agreement in the neighborhood of the minimum points should be noted. The reason that the M-diffusion result is not included for comparison is that it gives areas that always lie above the J-diffusion result. No attempt was made to find the best fit parameters for the Fixman–Rider generalization[12] of Gordon's theory for the same reason. This will be discussed in the next section. Suffice it to say that the generalized extended diffusion model can not be made to fit the results.

TABLE II. Time constants from dynamics in reduced units.

$\hat{\rho}$ (Relative to close packed)	$\dfrac{1}{\tau_c^*}$ (Enskog)	$\dfrac{1}{\tau_v^*}$ (Enskog)	$\dfrac{1}{\tau_v^*}$ (Area)	$\dfrac{1}{\tau_\omega^*}$ (Enskog)	$\dfrac{1}{\tau_\omega^*}$ (Area)	β_1 (Opt)	β_2 (Opt)	τ_1^* (Dyn)	τ_2^* (Dyn)
0.100	0.382	0.329	0.341	0.174	0.176	0.289	0.306	1.82	0.887
0.200	0.954	0.822	0.840	0.455	0.420	0.531	0.504	1.25	0.632
0.270	1.49	1.29	1.27	0.694	0.621	0.778	0.824	1.11	0.572
0.333	2.11	1.81	1.74	0.994	0.903	0.734	0.615	1.04	0.552
0.400	3.14	2.69	2.83	1.49	1.30	0.849	0.648	1.19	0.604
0.500	5.19	4.46	5.32	2.48	2.10	1.48	1.15	1.40	0.675
0.555	6.46	5.71	7.35	3.01	2.43	1.87	1.28	1.48	0.729
0.625	9.62	8.03	15.0	4.38	3.71	3.18	3.02	1.92	0.831
0.666(l)	12.0	10.1	24.3	5.59	4.52	4.15	4.15	2.45	1.04
0.666(s)	8.93	7.60	89.3	4.42	3.48	3.21	3.06	1.97	0.837

The optimized values of β were determined using the procedure outlined in connection with Eq. (2.14). The first 80 points of $C_l^{\text{expt l}}(\tau)$ were used, and the optimized value of β_l is that value that minimizes the deviation $\Delta_l(T, \beta)$. These values are then used to compute the orientational correlation functions in the Gordon J-diffusion model. This is done by Laplace inverting Eq. (2.8b). An algorithm was developed using the IBM SSP fast Fourier transform routine. 500 Fourier coefficients proved sufficient to do all the work here. A comparison between the experimental $C_1(\tau)$ and $C_2(\tau)$ and those predicted using the Gordon theory is presented in Figs. 2 and 3.

The same fast Fourier transform procedure was followed in evaluating the extended diffusion model in the Enskog approximation[11] as evaluated by Chandler [cf. Eqs. (3.17)–(3.19)]. The values of β were evaluated using Eq. (3.17) and thus come directly from column 5 of Table II. A comparison between experiment and the orientational correlation function predicted on the basis of the Enskog theory[11] is presented in Figs. 2 and 3. The disagreement between the theory and experiment is larger than the possible uncertainty in the experimental results. The experimental uncertainty is of the order of ± 0.02 (see below).

To compare the Fokker–Planck theory[12,13] with molecular dynamics, we followed the following prescription. According to Eq. (2.21a), $C_\omega(\tau)$ should decay exponentially in time with a rate of decay β. However, this exponential decay should not be taken literally. Rather, it represents the angular velocity correlation function in a coarse grained sense. Thus, we choose the value of β such that we get the correct zero-frequency value; that is,

$$\beta^{-1} = \tau_\omega^*(\text{area}) .$$

[If we chose the literal interpretation of the exponential decay, then $\beta^{-1} = \tau_\omega^*(\text{slope})$.] As a result, the Fokker–Planck theory requires one parameter which must be extracted from the experimental data and is not calculable from theory. The values to be used in the Fokker–Planck theory are thus readily found in column 6 of Table II. Fortunately, Fixman and Rider[12] have developed algorithms for computing $C_l(\tau)$ for each of the values of β. The results of their calculation are compared with dynamics in Fig. 4. The excellent agreement should be noted. For very large values of β, the Fokker–Planck theory should reduce to the Debye model of small step diffusion with a rotational diffusion coefficient D_r^* (in reduced units),

$$D_R^* = \beta^{-1} = \tau_\omega^*(\text{area}).$$

Thus, if the Debye model is valid, $C_l(\tau)$ should decay as $\exp - l(l+1)D_R^*\tau$. A comparison of the Debye model[8] with dynamics is also presented in Fig. 5 only for those states for which it is in reasonable agreement. There is no sense comparing this theory to the observed highly nonexponential functions. The areas under the correlation functions $C_1(\tau)$ and $C_2(\tau)$ predicted on the basis of the Fokker–Planck theory are plotted vs $\beta \equiv 1/\tau_\omega^*(\text{area})$ in Fig. 1. For the sake of comparison, the measured values of τ_l^* are also plotted vs $1/\tau_\omega^*(\text{area})$. The excellent agreement for sufficiently high values of $1/\tau_\omega^*(\text{area})$ should be noted.

The various orientational correlation times are presented in Table III.

VI. DISCUSSION

It is clear from Fig. 5 that the angular velocity correlation function deviates positively from the Enskog correlation function, Eq. (3.14b). This positive deviation grows with density over the whole range of fluid densities and indicates that even at low densities, correlated collisions play an important role—so much so, in fact, that simple models of reorientations based on independent binary collision theory such as the Enskog model developed by Chandler[11] cannot describe the results. This positive deviation indicates a persistence of angular velocity which may have its aetiology in hydrodynamic effects according to which $C_\omega(t) \sim t^{-(d+2/2)}$, where d is the dimensionality of the system.[26] So far, there is no indication that this is the case, but we are currently involved in a rather extensive exploration of this problem. Several points must be considered in connection with the positive deviation. First, it is not obvious that the deviation should be positive. The linear velocity correlation function of the rough sphere fluid is also shown in Fig. 5. It is important to note that this function deviates negatively from the Enskog correlation function [cf. Eq. (3.14b)] and at high fluid densities
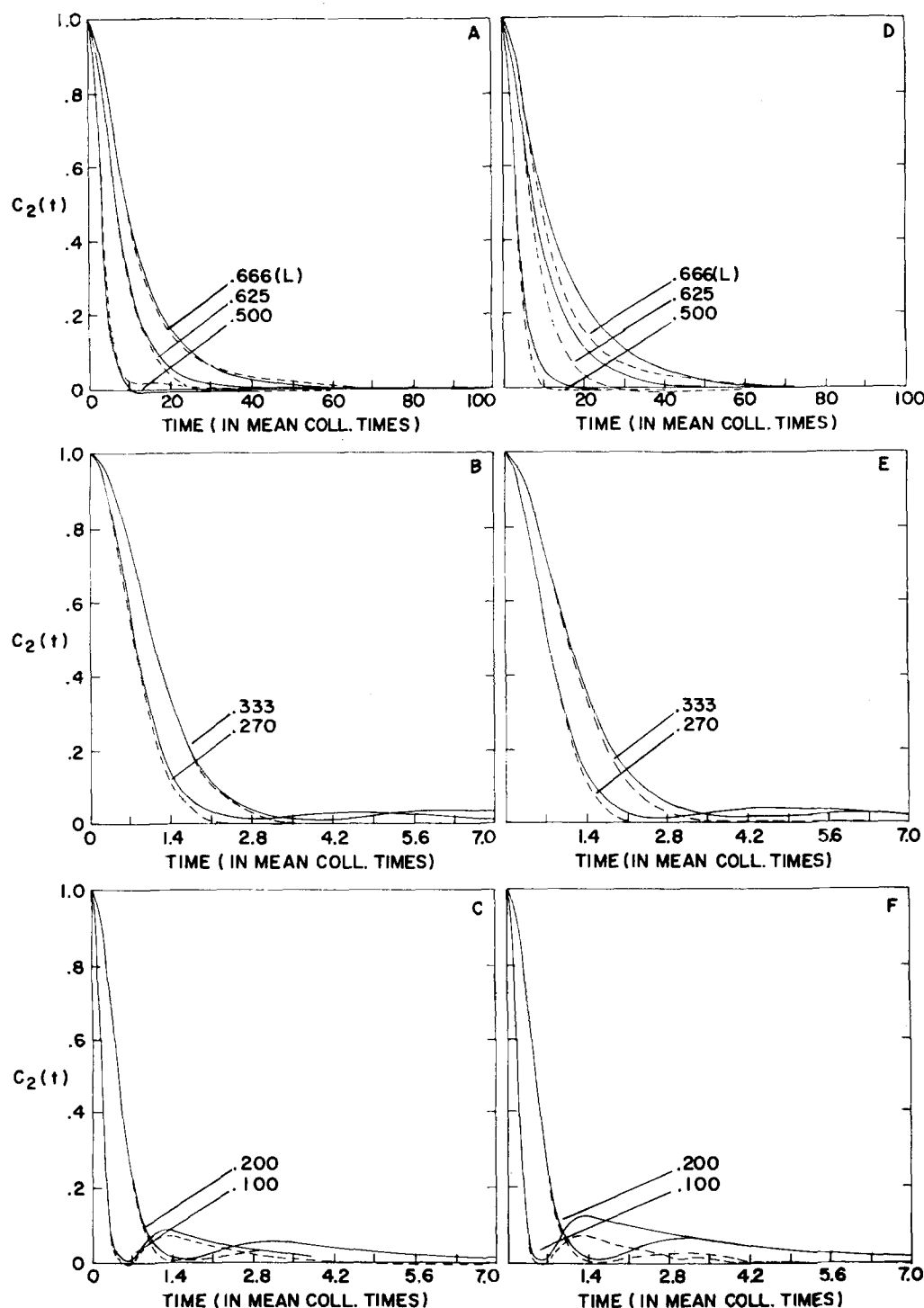
FIG. 3. See Fig. 2 for description of symbols. This graph for C_2's uses the same notation.

become negative. This is entirely consistent with the observed density dependence of the velocity correlation functions in the smooth hard sphere fluid, and in the Lennard-Jones fluid. Thus, in a rough sphere fluid, as the density increases the angular velocity correlation function deviates more and more positively from the Enskog theory, whereas the linear velocity correlation function deviates more and more negatively from the Enskog theory. This stands in marked contrast to molecular dynamics (and other experiments) on fluids contain-

ing anisotropic molecules[27] where the behavior of the angular velocity is much like the linear velocity—with its high density negative deviation. In these fluids the cage effect is thought to be responsible for the fact that on the average a collision reverses both the angular and linear velocity, thereby leading to a negative region in both the vcf and the avcf at sufficiently high densities. The positive deviation of $C_\omega(t)$ in the rough sphere fluid even at the melting density is therefore quite unexpected—and has yet to be explained on theoretical
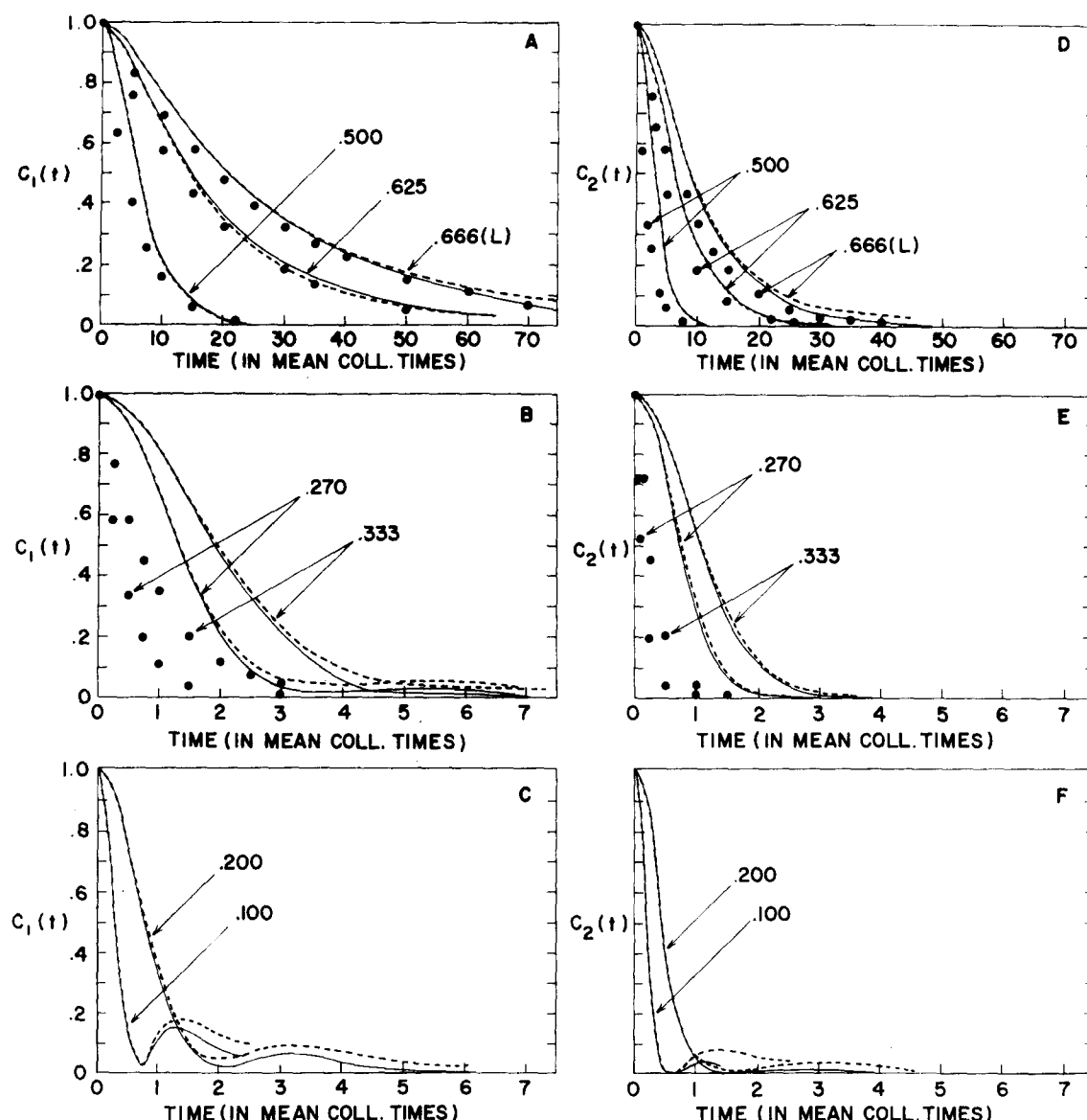
FIG. 4. The orientational correlation functions $C_1(\tau)$ and $C_2(\tau)$ vs the time in units of the collision time at different densities. Dashed lines are the dynamics data. The solid lines are the curves predicted by the Fokker–Planck model. The dots are the correlation functions predicted by the rotational diffusion model.

grounds.

It is important to note that if $C_\omega(t)$ deviates positively from the Enskog theory—that is, if there is a persis-

tence of angular velocity, the fluid behaves more like a collection of free rotors (where the avcf stays constant), and the orientational correlation functions should decay faster. Thus, in general, we should expect the $C_1(\tau)$

TABLE III. Orientational correlation times.

| $\hat{\rho}$	τ_1^* (Dyn)	τ_1^* (F–P)[1]	τ_1^* (Opt)	τ_1^* (Enskog)	τ_2^* (Dyn)	τ_2^* (F–P)[1]	τ_2^* (Opt)	τ_2^* (Enskog)
0.100	1.815	1.50	2.05	3.09	0.887	0.600	0.997	1.55
0.200	1.25	1.07	1.45	1.55	0.632	0.538	0.745	0.790
0.270	1.11	1.02	1.30	1.33	0.572	0.542	0.664	0.680
0.333	1.04	1.03	1.32	1.29	0.552	0.555	0.701	0.650
0.400	1.19	1.11	1.29	1.37	0.604	0.582	0.692	0.670
0.500	1.40	1.37	1.36	1.69	0.675	0.653	0.651	0.770
0.555	1.48	1.50	1.48	1.91	0.729	0.686	0.657	0.834
0.625	1.92	2.05	1.97	2.49	0.831	0.831	0.835	1.00
0.666(l)	2.45	2.42	2.38	3.04	1.04	0.935	0.979	1.18
0.666(s)	1.97	1.95	1.98	1.91	0.837	0.802	0.839	1.02
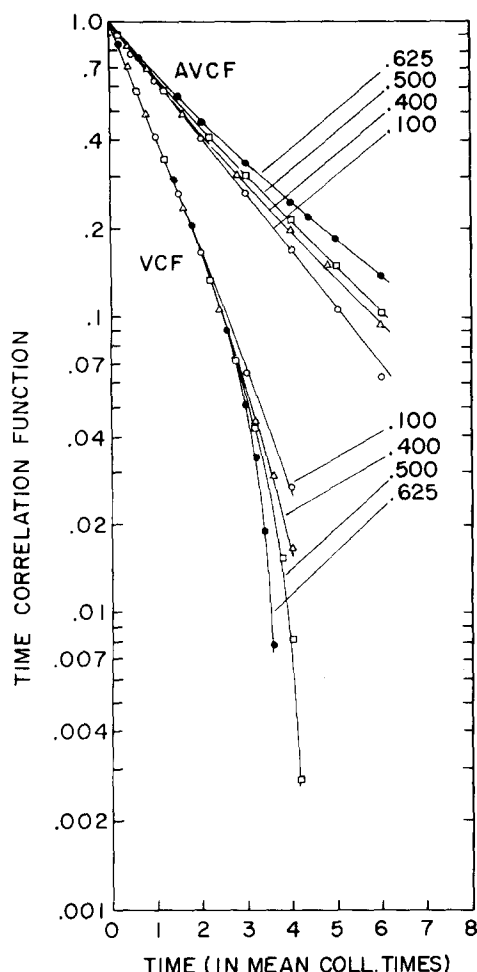
FIG. 5. The angular and linear velocity correlation functions showing, respectively, the positive and negative deviations from the Enskog result. In both cases the lowest density shown (0.100) is coincident with an Enskog exponential curve.

ly argues against the viability of the J-diffusion model.[10] This model fails to give the correct $C_\omega(t)$ and in addition fails to give the correct orientational correlation times. As is clear from Figs. 2 and 3, the J-diffusion model also fails to give the detailed time dependence of the $C_l(\tau)$ for those densities for which it also fails to give the correct orientational correlation times. Despite this, at high densities it is possible to find values of β for which agreement can be achieved, but the value of β which is optimum for $C_1(\tau)$ (denoted by β_1) is not necessarily the same as that for $C_2(\tau)$ (denoted by β_2). This is clearly seen in Table II. Nevertheless, the differences between β_1 and β_2 may not be large enough to say categorically, given the experimental error, that there is no self-consistency in the theory. From the above, it is clear that the J-diffusion model is qualitatively useful but is incapable of correctly giving $C_l(\tau)$ at intermediate densities and, moreover, cannot simultaneously give both $C_\omega(\tau)$ and $C_l(\tau)$. In addition, the optimum values of β_1 and β_2 neither agree with each other nor (more seriously) do they seem to have anything to do with the collision time (see Table II).

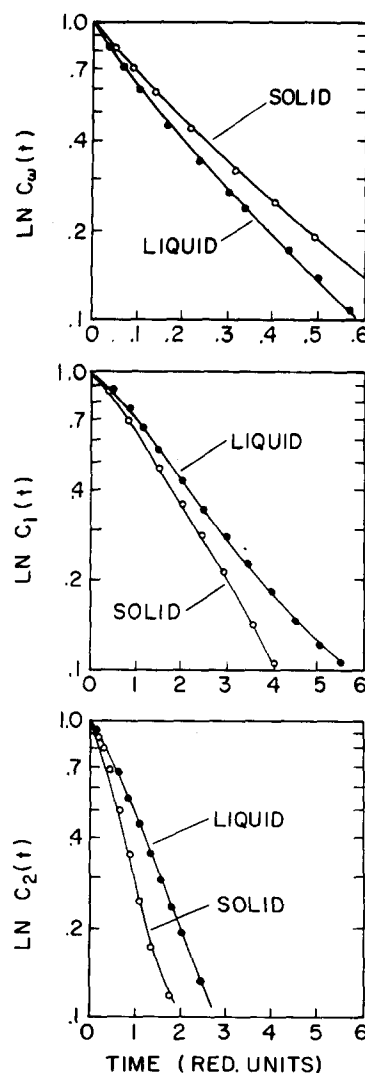The Enskog theory as advanced by Chandler[11] also fails. First, the angular velocity correlation function

to decay more rapidly than would be predicted by the Enskog theory. This is clearly evident in Figs. 2 and 3.

As was pointed out, the rough sphere system has a melting transition at $\hat{\rho} = 0.666$. The $C_\omega(t)$ for the fluid and solid at this density are presented in Fig. 6. Figure 6 indicates that in the solid, $C_\omega(\tau)$ decays more slowly than in the fluid. In fact, the positive deviation from the Enskog result is less for the solid than for the fluid. Thus, it would appear that the spheres tumble more freely in the solid than in the liquid, a fact consistent with the larger collision frequency in the liquid. This conclusion is also reflected in Fig. 6, where the orientational correlation functions $C_1(\tau)$ and $C_2(\tau)$ for the fluid and solid are compared. Thus, we conclude that rough spheres tumble more freely in the solid than the liquid state.

Comparing the orientational correlation times τ_l^* predicts on the basis of the J-diffusion model [cf. Eq. (2.13a)] with dynamics in Fig. 1 and Table III, we see that there are densities for which the optimized β's yield τ_l^* which are larger than the experimental correlation times. In fact, there are no β's for which the theory can give several of the observed τ_l^*. This clear-

FIG. 6. A semilog plot of $C_\omega(t)$, $C_1(t)$, and $C_2(t)$ for the distinct fluid and solid phases that could be equilibrated at the density 0.666.

deviates positively from the Enskog approximation. Secondly, a plot of the experimental τ_l^* vs $1/\tau_\omega^*{}_{(Ensk)}$ deviates considerably from the theoretical curve. This is indicated in Tables II and III, and in Fig. 1. Thirdly, the predicted orientational correlation functions, as indicated in Figs. 2 and 3, are out of line with the experimental curves. It is clear that the set of plausible assumptions that were made by Chandler do not suffice for a description of orientational relaxation.

Chandler has pointed out[28] that his derivation of the J-diffusion model is actually the unique microscopic derivation of that theory. This fact is easily understood in view of Eq. (3.18a). There is only one truncation of the cumulant series which yields the J-diffusion model result that $K_l(t)$ is $K_l^{(0)}(t)$ times an exponential. Thus, Chandler's Enskog theory actually removes the adjustability of the parameter β in the J-diffusion model, and any criticism of the Enskog theory is also a criticism of the J-diffusion model. However, experimental work frequency treats β as adjustable. For this reason we have also presented a test of the J-diffusion model independent of Chandler's microscopic analysis.

There is evidence that a good approximation to the memory function $K_l(\tau)$ introduced in Eq. (3.18a) is

$$K_l(t) = K_l^{(0)}(t)\, C_\omega(t)\ ,$$

where $K_l^{(0)}(t)$ is the free particle memory function and $C_\omega(t)$ is the experimentally determined correlation function. Nevertheless, for this to be useful there must be a theoretical determination of $C_\omega(t)$, a theory that does not presently exist.

The M-diffusion and the generalized extended diffusion models of Fixman and Rider are less satisfactory than the J-diffusion model because for all values of $\beta = \beta_0 + \beta_1$, $C_l(\tau)$ would decay even more slowly in these models than does the J-diffusion model.

The only theory that has any success at moderate and high densities is the Fokker–Planck theory, but this also fails at low densities. These conclusions are borne out by Fig. 4, where the excellent agreement between the theoretical and the experimental $C_l(\tau)$ is displayed. In addition, the orientational correlation times also agree, as is evident in Fig. 1 and in Table III. It is also clear from Fig. 4 that the Fokker–Planck theory
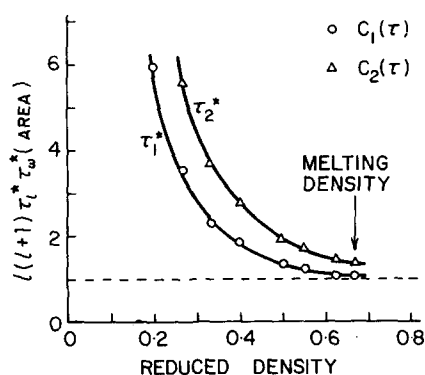
reduces to the Debye model only at the very highest densities. The friction constant was chosen such that the correct τ_ω^*(area) is achieved. The rotational diffusion coefficient then turns out to be $D_{\text{rot}}^* = \tau_\omega^*$(area). The Fokker–Planck theory is not very successful at low densities. It is quite possible that a Fokker–Planck equation with memory would work:

$$\left[\frac{\partial}{\partial t} + i\omega \cdot I\right] P(t) + \int_0^t dt\, \Phi_\omega(t-\tau)\nabla_\omega \cdot \left[\nabla_\omega + \frac{I}{kT}\,\omega\right] P(\tau) = 0\ ,$$

where P is the joint probability distribution function defined immediately following Eq. (2.19a), and $\Phi_\omega(\tau)$ is the experimental angular velocity memory function. This is a very difficult equation to solve and is also useful only if $\Phi_\omega(t)$ can be independently determined.

In conclusion, no model known to the authors has yet been devised which explains even the simplest single particle orientational correlation functions over the complete range of fluid densities. Most of the problems seem to arise at densities such that inertial effects are comparable with collisional effects. This is somewhat surprising, since it is precisely in this density regime that we would have expected the extended diffusion models to work. It appears that even at the lowest densities, the Enskog theory works less well for orientational relaxation than it does for the linear and angular velocity correlation function.

The high density–Hubbard relation[14] [see Eq. (3.21)] was tested by plotting $l(l+1)\tau_l^*\tau_\omega^*$(area) vs the density. The result is shown in Fig. 7. It is clear that if the Hubbard relation is valid, then at high densities the curve should approach unity for both $l=1$ and $l=2$. For $l=1$ this seems to happen at densities ≥ 0.625, whereas for $l=2$ it can happen only for densities >0.666, which is the melting density. We conclude that the Hubbard relation[14] is not valid for the rough sphere model at fluid densities. It is expected that this relation may account for the behavior in metastable superdense fluids, but we have not pursued this matter here.

In conclusion then, we emphaize the following points concerning the rough sphere system:

(a) Particles rotate more freely in solid than in the liquid phase at the melting density. In addition, the deviation from Enskog in $C_\omega(t)$ decreases from liquid to solid and in $C_v(t)$ increases from liquid to solid.

(b) As in the smooth sphere fluid, $C_v(\tau)$ deviates negatively, whereas $C_\omega(\tau)$ deviates positively from the Enskog results. These deviations grow with density, but the deviation in $C_\omega(\tau)$ seems to arise at lower density than that in $C_v(\tau)$. These deviations reflect the importance of correlated binary collisions and, at least for $C_\omega(\tau)$, these occur even at low densities.

(c) The J-diffusion model is incapable of accounting for several features of these experiments. First, only at sufficiently high densities can parameters β be found which give reasonable $C_l(\tau)$, but even then these values of β can in no way be interpreted as the collision rate. In addition, the β's which are optimum for C_1 are not optimum for C_2. More importantly, no β's can be found

FIG. 7. Test of the Hubbard relation [cf. Eq. (3.21)] using the relaxation time of $C_\omega(t)$ defined by its time integral.

for densities for which inertial effects are comparable to collisional effects which simultaneously give agreement with the observed $C_1(\tau)$ or with the observed orientational correlation times. In addition, the optimized choice of β even at high densities does not appear to be given by the collision time as required by Gordon's formulation, nor is it given by the angular velocity correlation time in the Enskog approximation as would be required by the Chandler theory.

(d) Any extended diffusion model intermediate between the M- and J-diffusion model gives even worse agreement than the J-diffusion model.

(e) The Enskog theory advanced by Chandler does not agree with experiment even at low fluid densities where we expect the Enskog approximation to be valid.

(f) The model which seems to agree with experiment over the widest range of densities is the Fokker–Planck theory. This model does not describe with accuracy the range of densities for which the inertial and collisional effects are of the same magnitude. The data do not go to sufficiently small densities, but we suspect that the Fokker–Planck theory will not work for rarified fluids.

(g) The small step diffusion model seems to give approximate agreement only at the two highest fluid densities studied.

(h) The high density Hubbard relation does not seem to be valid at any stable fluid density.

Since almost all the theories outlined in this paper are Markoffian theories,[12] their failure at low densities may indicate the failure of the Markoffian theory.

It is important to note that the rough sphere fluid is a highly idealized model which probably underestimates the collisional effects on the angular decay that are present in anisotropic fluids. For example in real fluids, the rotation of anisotropic molecule can involve the displacement of neighboring molecules; that is, free volume must be present for the molecule to tumble. This is not required in the rough sphere fluid where molecules have exact spherical symmetry. Nevertheless, it would not be surprising if some spherical tops like CH_4 or CCl_4 were to exhibit similar properties to the rough sphere fluid. Needless to say, to compare these systems to the rough sphere fluid, the appropriate value of κ must be used, and we have studied only the case of $\kappa = 0.4$. There may be interesting dynamical effects at different values of κ, a subject we leave for future study. In addition, it is not difficult to change the roughness of the sphere. Since we have been dealing here with the roughest possible sphere, we do not think that lessening the roughness will bring the model closer to real systems.

Needless to say, there is always some experimental error in a molecular dynamics study. We have run five different runs on the density 0.3333 and find from the normal error analysis that our curves are good to within a few percent. This conclusion is also borne out by Table I, in which the initial slopes are compared with "exact" initial slope. In addition, three different runs of 10 800 collisions were made at density 0.500. In
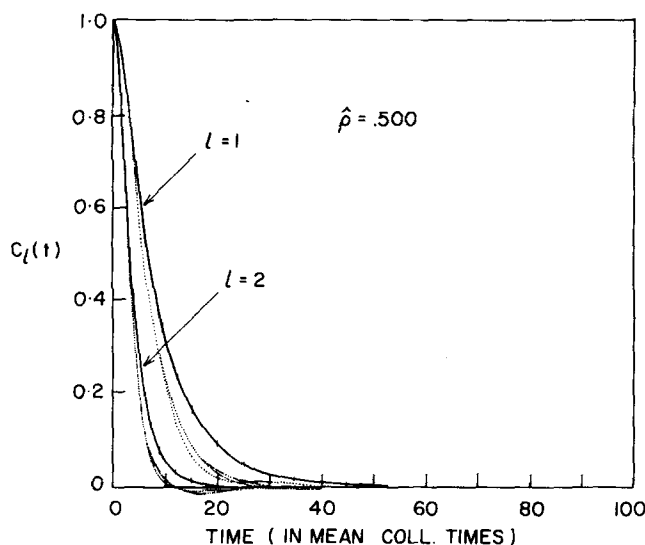

FIG. 8. Comparison of three different dynamics experiments at $\beta = 0.500$. The dots are the results of the experimental C_l's and the solid lines are the Enskog correlation functions. The error bars indicate the spread in the initial slopes in $C_\omega(\tau)$.

Fig. 8 the orientational correlation functions $C_1(\tau)$ and $C_2(\tau)$ for these three runs are compared with the Enskog theory. The Enskog curves were computed using the three different slopes $1/\tau_\omega^*$(slope) from the dynamics. These curves clearly show that there is a discernable difference between theory and experiment.

Although the accuracy can be improved by studying either a larger system or by running a longer trajectory, we are confident that our conclusions are correct. To improve our accuracy by a factor of 10, our computer use would have had to be increased by a factor of 100, from 5 h to 500 h. We are presently involved in a very elaborate study of long time tails in the rotational relation of rough spheres and ellipsoidal molecules.

ACKNOWLEDGMENTS

[1] J. D. Weeks, D. Chandler, and H. C. Andersen, J. Chem. Phys. 54, 5237 (1971); 55, 5422 (1971).
[2] J. Kushick and B. J. Berne, J. Chem. Phys. 59, 3732 (1973).
[3] See W. Wood (preprint); see citations to Alder and Wainwright.
[4] M. H. Ernst, E. H. Hauge, and J. M. van Leeuwan, Phys. Rev. Lett. 25, 1254 (1970).
[5] J. R. Dorfman and E. G. D. Cohen, Phys. Rev. Lett. 25, 1257 (1970).
[6] There has been considerable work on the kinetic theory of rough sphere gases. See, for example, E. W. Condiff, Weu-Kao Lu, and J. S. Dahler, J. Chem. Phys. 42, 3445 (1965); B. J. McKoy, S. I. Sandler, and J. S. Dahler, J. Chem.

Phys. 45, 3485 (1966).

[7]See, for example, the discussion given by S. Chapman and T. G. Cowling, *The Mathematical Theory of Non-Uniform Gases* (Cambridge U. P., Cambridge, 1960).

[8]P. Debye, *Polar Molecules* (Dover, New York, 1969).

[9]E. N. Ivanov, Sov. Phys. JETP 18, 1041 (1964).

[10]R. G. Gordon, J. Chem. Phys. 44, 1830 (1966).

[11]D. Chandler, J. Chem. Phys. 60, 3508 (1974).

[12]M. Fixman and K. J. Rider, J. Chem. Phys. 51, 2425 (1969).

[13]P. S. Hubbard, Phys. Rev. A 6, 2421 (1972), and references cited therein to the work of Condiff, Dahler, and Steele.

[14]P. S. Hubbard, Phys. Rev. 131, 1155 (1963).

[15]The extension of the M-diffusion and J-diffusion model to spherical tops was made by R. E. W. McClung, J. Chem. Phys. 51, 3842 (1969).

[16]B. J. Berne in *Physical Chemistry*, edited by H. Eyring, D. Henderson, and W. Jost (Academic, New York, 1971), Sec. XIIIB, p. 539.

[17]M. Fixman (private communication).

[18]See, for example, J. Hirschfelder, C. Curtis, and R. Bird, *Molecular Theory of Gases and Liquids* (Wiley, New York, 1954).

[19]N. F. Carnahan and K. E. Starling, J. Chem. Phys. 51, 635 (1969).

[20]For a simple didactic introduction, see R. Zwanzig, Ann.

Rev. Phys. Chem. 16, 67 (1965), and for a more recent review see B. J. Berne and D. Forster, Ann. Rev. Phys. Chem. 22, 563 (1971).

[21]R. Kubo, J. Chem. Phys. 44, 1830 (1962).

[22]D. Chandler, J. Chem. Phys. 60, 3500 (1974).

[23]This conclusion follows from the fact that successive uncorrelated binary collisions lead to $\kappa_n = 0$ for $n = 2, 3\cdots$. This is a consequence of a theorem due to Kubo (see Ref. 21).

[24]R. Zwanzig, Phys. Rev. 129, 486 (1963). Also, for a detailed discussion of the binary collision expansion for hard sphere systems, see M. H. Ernst, J. R. Dorfman, W. R. Hoegy, and J. M. Van Leeuwen, Physica (Utr.) 45, 127 (1969).

[25]For the density $\hat{\rho} = 0.555$, the unit vectors were sampled randomly with respect to the $\hat{\omega}$ ten different times. The resulting C_1's and C_2's varied by no more than 2%.

[26]B. J. Berne, J. Chem. Phys. 56, 2165 (1972), N. K. Ailawadi and B. J. Berne, J. Chem. Phys. 54, 3569 (1970); N. K. Ailawadi and B. J. Berne, Conf. Stat. Mech., I. U. P. A. P., Chicago, 1971 (1972), p. VI. 22.

[27]B. J. Berne and G. Harp, Adv. Chem. Phys. 22, 63 (1970); J. Kushick and B. J. Berne, J. Chem. Phys. 59, 4486 (1973).

[28]D. Chandler (private communication).